Development/Plasticity/Repair

In Vivo Calcium Signaling during Synaptic Refinement at the *Drosophila* Neuromuscular Junction

Fernando Vonhoff and Haig Keshishian

Molecular, Cellular, and Developmental Biology Department, Yale University, New Haven, Connecticut 06520

Neural activity plays a key role in pruning aberrant synapses in various neural systems, including the mammalian cortex, where low-frequency (0.01 Hz) calcium oscillations refine topographic maps. However, the activity-dependent molecular mechanisms remain incompletely understood. Activity-dependent pruning also occurs at embryonic *Drosophila* neuromuscular junctions (NMJs), where low-frequency Ca^{2+} oscillations are required for synaptic refinement and the response to the muscle-derived chemorepellant Sema2a. We examined embryonic growth cone filopodia *in vivo* to directly observe their exploration and to analyze the episodic Ca^{2+} oscillations involved in refinement. Motoneuron filopodia repeatedly contacted off-target muscle fibers over several hours during late embryogenesis, with episodic Ca^{2+} signals present in both motile filopodia as well as in later-stabilized synaptic boutons. The Ca^{2+} transients matured over several hours into regular low-frequency (0.03 Hz) oscillations. *In vivo* imaging of intact embryos of both sexes revealed that the formation of ectopic filopodia is increased in *Sema2a* heterozygotes. We provide genetic evidence suggesting a complex presynaptic Ca^{2+}-dependent signaling network underlying refinement that involves the phosphatases calcineurin and protein phosphatase-1, as well the serine/threonine kinases CaMKII and PKA. Significantly, this network influenced the neuron's response to the muscle's Sema2a chemorepellant, critical for the removal of off-target contacts.

Key words: activity-dependent; chemorepulsion; filopodia; live imaging; oscillations; pruning

---

Significance Statement

To address the question of how synaptic connectivity is established during development, we examined the behavior of growth cone filopodia during the exploration of both correct and off-target muscle fibers in *Drosophila* embryos. We demonstrate that filopodia repeatedly contact off-target muscles over several hours, until they ultimately retract. We show that intracellular signals are observed in motile and stabilized "ectopic" contacts. Several genetic experiments provide insight in the molecular pathway underlying network refinement, which includes oscillatory calcium signals via voltage-gated calcium channels as a key component. Calcium orchestrates the activity of several kinases and phosphatases, which interact in a coordinated fashion to regulate chemorepulsion exerted by the muscle.

Introduction

Understanding the cellular and molecular mechanisms that govern the formation of neural circuits is a major goal of developmental neurobiology. The initial stages of axon guidance and target recognition involve multiple chemotropic signals that may be either attractive or repulsive (for review, see Kolodkin and Tessier-Lavigne, 2011). Early off-target contacts are removed during a subsequent period of synaptic refinement or pruning (Katz and Shatz, 1996; Doll and Broadie, 2014). Synaptic pruning typically involves mechanisms that are activity-dependent (Flavell and Greenberg, 2008), but the molecular pathways remain incompletely resolved. The mechanisms governing synaptic pruning are of clinical interest, given recent studies implicating either excessive or inadequate synaptic pruning in disorders such as schizophrenia and autism (Berridge, 2012; Tang et al., 2014; Sekar et al., 2016).

The *Drosophila* neuromuscular junction (NMJ) has served as a powerful genetic model system for studying network development and synaptic plasticity (Ruiz-Cañada and Budnik, 2006; Menon et al., 2013). The connections between embryonic *Drosophila* motoneurons and body wall muscle fibers are stereo-

typic, making the detection of wiring errors straightforward (Jarecki and Keshishian, 1995; Chang and Keshishian, 1996). *Drosophila* motoneuron growth cones initially contact multiple off-target muscle fibers (Halpern et al., 1991; Sink and Whitington, 1991; Chiba et al., 1993) that must be withdrawn during an early critical period, or they will mature into functional ectopic synapses (Jarecki and Keshishian, 1995). Synaptic refinement at the *Drosophila* NMJ requires presynaptic electrical activity (White et al., 2001; Carrillo et al., 2010; Vonhoff and Keshishian, 2017a) and a trans-synaptic retrograde chemorepulsive signal from the muscle fiber, mediated by Semaphorin2a (Sema2a) (Matthes et al., 1995; Winberg et al., 1998; Carrillo et al., 2010).

Calcium is a key second messenger that orchestrates a variety of intracellular signaling cascades and axon guidance mechanisms (Gomez et al., 2001; Rosenberg and Spitzer, 2011). At the developing *Drosophila* NMJ, Ca^{2+} influx leads to the activation of at least two Ca^{2+}-dependent signaling systems that are required for the removal of off-target neuromuscular contacts: the Ca^{2+}-dependent kinase CaMKII (Carrillo et al., 2010) and the Ca^{2+}-dependent adenylyl cyclase Rutabaga (Vonhoff and Keshishian, 2017a). A remarkable feature of the Ca^{2+} and cAMP signaling is that both involve episodic activity in the range of 0.01 Hz (Carrillo et al., 2010; Vonhoff and Keshishian, 2017a). Activity waves have been widely observed during the development of various neural systems, including the mammalian visual system (Meister et al., 1991; Penn et al., 1998; Ackman et al., 2012), *Xenopus* spinal cord (Gomez and Spitzer, 1999; Gomez et al., 2001), and chick motoneurons (Hanson and Landmesser, 2004; Hanson et al., 2008). However, the molecular means by which activity oscillations refine neuronal networks are still not completely resolved.

Using *in vivo* imaging of singly identified motoneuron growth cones and synapses, we have examined the cellular and molecular mechanisms that underlie the pruning and refinement of *Drosophila* NMJs. These results include an analysis of Ca^{2+} signaling and the development of low-frequency oscillatory Ca^{2+} activity within embryonic growth cones. Examining growth cone dynamics, we characterize the role of the muscle-derived chemorepellant Sema2a in influencing filopodial exploration and contacts onto on- and off-target muscle surfaces.

As noted above, synaptic refinement at the NMJ involves the presynaptic activity of both CaMKII and Ca^{2+}-dependent adenylyl cyclase (Carrillo et al., 2010; Vonhoff and Keshishian, 2017a). To identify other signaling systems in the neuron that may be involved in synaptic refinement, we used genetic approaches to analyze the role of calcineurin (CaN) and its genetic interactions within the molecular pathway underlying refinement. Moreover, a locus encoding the mammalian CaN γ catalytic subunit has been associated with susceptibility to schizophrenia (Gerber et al., 2003; Liu et al., 2007) and CaN knock-out in the mouse forebrain leads to schizophrenia-like behavior (Miyakawa et al., 2003), suggesting a possible link between CaN, aberrant refinement, and schizophrenia. Collectively, our studies advance our understanding of how refinement is regulated in a system of singly identifiable synapses, leading to precise synaptic connectivity during development.

Materials and Methods

Fly stocks. We thank the following organizations and individuals for providing stocks: Bloomington Stock Center: elav[C155]-GAL4(BL458), UAS-GFP(BL35786), UAS-GCaMP5(BL42037), UAS-myr-TdTomato(BL32223), UAS-CD8-GFP(BL5137), *Dmca1G[null]*(BL51994), UAS-Dmca1G-RNAi (BL39029), UAS-Dmca1D-RNAi(BL33413), UAS-CanA-14D-RNAi

(BL25929), UAS-CanB-RNAi(BL27301), UAS-CanB2-RNAi(BL38971), *CanA-14D[LOF]*(BL22025), *CanA-14F[LOF]*(BL17478), *CanA1[LOF]*(BL42342), *CaMKII[LOF]*(BL60770), UAS-CaMKII[R3](BL29662), UAS-CaMKII[T287A] (BL29663),UAS-CaMKII[T287D](BL29665),*rut[1]*(BL9404),*pp1a96A[2]*(BL23698), UAS-pp1a96A[2](BL23700). Vienna Drosophila Resource Center: UAS-cacophony-RNAi(5551), UAS-Dmca1D-RNAi(51491), UAS-Ca-Ch-β-RNAi(27581), UAS-CanA-14F-RNAi(30105), UAS-CanA1-RNAi(32283). Kyoto Stock Center: UAS-CanA14D-WT(109868) (Nakai et al., 2011), UAS-CanA14D-H217Q(109869), UAS-CanA14act(116255). R. Ordway, Pennsylvania State, State College: UAS-cac1-eGFP-786C. T. Littleton, Massachusetts Institute of Technology and D. K. O'Dowd, University of California–Irvine: *cac[TS3]*, *cac[NT27]* (Rieckhof et al., 2003). A. Kolodkin, Johns Hopkins Medical School: *Sema2a[B65]*(Wu et al., 2011), *PKAR2[LOF]* (*PKAR2[EP(2)2162]*; Park et al., 2000), UAS-PlexinB (Hu et al., 2001). L. Griffith, Brandeis University: UAS-CaMKII[NTide] (Haghighi et al., 2003) C. F. Wu, University of Iowa: *dnc[M11]*. A. DiAntonio, Washington University: MHC-Sh-CD8-GFP (Zito et al., 1999). The isogenic line Canton-S 5 (CS5) was used as control. As previously described for UAS-PKA[act] (Vonhoff and Keshishian, 2017a), UAS-CanA14D[act] was expressed using the elav-GeneSwitch-GAL4 driver (Osterwalder et al., 2001). Flies were reared at 25°C, except of *cac* flies, which were reared at room temperature (~22.5°C).

Experimental design and statistical analysis. For each experiment, the genotype of the control group and sample size are described in the legend of the corresponding figure. Unless otherwise stated in the text, animals of both sexes were examined, and no significant differences were detected on the basis of gender, so the data were therefore pooled. Power analysis was calculated using GPower software 3.0.10 (University of Duesseldorf) (Faul et al., 2007), and a sample size for ectopic counts of $n = 9$ animals for an α level of 0.05 and a power level of 0.8 was calculated as previously shown (Vonhoff and Keshishian, 2017a). Statistical significance was calculated using ANOVA or *t* test, using Prism-6-Software (GraphPad Software).

Imaging filopodial motility and Ca transients. Imaging of intact embryos was performed using a Zeiss LSM880, with a 63× oil, 1.4 NA, and a 40× W, 1.3 NA objective using the super-resolution Airyscan acquisition and deconvolution mode, or a Bio-Rad1024, with a 40× oil, 1.3 NA objective. For motoneuron growth cone visualization, elav[C155]-GAL4 was used to express the membrane bound UAS-cd8-GFP or UAS-myr-TdTomato. For filopodial analysis, images were collected every 10 s for 10–100 min. Filopodial length was measured using ZEN (Zeiss Software) or Imaris (Bitplane). For Ca^{2+} imaging, embryos expressing UAS-GCaMP5 and UAS-myr-TdTomato using elav[C155] were imaged. One hour egg lays were set and incubated at 25°C. Embryos were manually dechorionated and mounted on coverslips in #700 halocarbon oil (Halocarbon Products). To suppress movement, we used embryos homozygous for a null mutation of the myosin heavy chain gene (*Mhc[1]*). *Mhc[1]* embryos have apparently normal neuromuscular development, forming presynaptic motoneuron boutons and localized postsynaptic receptors (see Fig. 1C). They also have normal condensation of the CNS (see Fig. 1A) and the presence of all peripheral nerves and muscles (see Fig. 1B). Late-stage wild-type (WT) embryos normally exhibit coordinated peristaltic movements along the length of the embryo (Pereanu et al., 2007; Crisp et al., 2008). Live GCaMP5 Ca^{2+} imaging of paralyzed, late-stage *Mhc[1]* embryos reveals the same coordinated peristaltic activity, but in the form of presynaptic Ca^{2+} signals at NMJs. This fictive activity indicates that, despite the *Mhc[1]*-induced paralysis, the central pattern generator required for intersegmental, coordinated motor activity is in place.

Data were collected from terminals of a single neuron, RP3, on muscles 7/6 in segment A3 as previously described (Vonhoff and Keshishian, 2017a) and analyzed using MATLAB (The MathWorks). Exponential-fit photobleaching correction algorithms were used to calculate F0 at each time point. Various image acquisition rates (3, 2, 1, and 0.5 Hz) were tested. At 2 Hz, we observed mean duration of 6.5 ± 0.5 s ($n = 11$ embryos, 68 transients) for Ca^{2+} transients. An acquisition rate of 1 image every 2 s (0.5 Hz) provided the best balance maximizing time resolution while minimizing photobleaching (see Fig. 3).

Analysis of ectopic contacts. NMJs from third instar larvae were analyzed as previously described (Berke et al., 2013). Ectopic contacts were

scored on muscles 7 and 6 in the abdominal segments A2-A7 and identified as previously described (Vonhoff and Keshishian, 2017a). Frequency of ectopic contacts is presented as mean ± SEM.

TrpA1 activation. Stage 16 embryos were stimulated in a PCR machine as previously described (Carrillo et al., 2010). All data were collected from male larvae hemizygous for elav-GAL4, expressing one copy of UAS-TrpA1 and either the corresponding CaMKII construct or in a *Sema2a*/+ background.

Fourier transform analysis. Oscillatory properties of embryonic Ca^{2+}-patterns were analyzed by fast Fourier transform nonlinear least-squares using Brass software version 3.0 (Biological Rhythm Analysis Software System; http://millar.bio.ed.ac.uk/PEBrown/BRASS/BrassPage.htm).

Results

Intracellular and episodic Ca^{2+} signals are detected within filopodia during the formation of motoneuronal contacts

During early embryonic development, motoneuron growth cones make multiple contacts with off-target muscles, withdrawing those connections as the NMJ matures (Halpern et al., 1991; Sink and Whitington, 1991; Chiba et al., 1993). However, a direct observation of filopodial exploration of off-target sites and possible Ca^{2+} signaling within the growth cones has yet to be examined. We imaged motoneuron growth cones at both on- and off-target muscles using time-lapse confocal microscopy of intact embryos. Using the genetically encoded Ca^{2+} indicator GCaMP, we also examined the intracellular Ca^{2+} signals present at these motile structures, as neurons explored the target domains.

To observe filopodial exploration at developing NMJs, we expressed membrane-tagged GFP in all motoneurons and imaged the dynamic behavior of the growth cones. Embryos were homozygous for Mhc^1 to suppress movements that would otherwise disrupt imaging (see Materials and Methods). We examined the growth cones exploring the four ventral longitudinal (VL) muscles 6, 7, 13, and 12. The muscles are principally contacted by axons projecting from the SNb nerve branch, but also receive transient contacts from adjacent nerve branches, notably the transverse nerve (TN) (Halpern et al., 1991; Chiba et al., 1993; Jarecki and Keshishian, 1995; White et al., 2001; Carrillo et al., 2010; Vonhoff and Keshishian, 2017a).

By 16.5 h after egg lay (AEL) (Campos-Ortega and Hartenstein, 1985; Pereanu et al., 2007) (embryonic Stage 17a), most motoneuron growth cones have arrived at their target innervation sites but still retain motile filopodia (Fig. 1D, D', magenta nerve). The TN includes motoneurons that normally innervate muscle 25 (located adjacent to muscles 7 and 6) and the alary muscle, as well as neurites from the lateral bipolar dendrite cell (Gorczyca et al., 1994). Although VL muscles are not normally innervated by TN motoneurons in WT animals, we repeatedly observed numerous motile filopodia emerging from the TN (Fig. 1D', blue nerve) in contact with ectopic sites on these muscles.

Filopodia emerging from the TN successively extended onto and retracted from the VL muscles 7 and 6 (Figs. 1D–H), on surfaces near the muscle fiber insertion site at the segment border, as opposed to the mid-muscle region where the native motoneuron innervation occurs (Halpern et al., 1991; Broadie and Bate, 1993; Chiba et al., 1993). The GFP-labeled TN filopodia had an average life-span of 15.3 ± 1.7 min and an average peak length of 3.6 ± 0.3 μm (n = 8 embryos, 93 filopodia scored). Repeated bouts of filopodial extension and retraction were detected at this ectopic muscle site over a window of several hours. This corresponds to the developmental period characterized as critical for synaptic refinement (Jarecki and Keshishian, 1995). In control embryos, the filopodial contacts usually failed to make the transition into stable ectopic NMJs (for an example of a transition of

an ectopic filopodial branch to a stabilized ectopic bouton-like structure, see Fig. 2A). This is in contrast to the previously described situation in embryos with blocked electrical activity, where ectopic TN-derived NMJs are frequently observed as stabilized synapses (Jarecki and Keshishian, 1995; White et al., 2001).

We next examined whether episodic intracellular Ca^{2+} transients were present in the TN-filopodia making contact with the VL muscles. Using GCaMP, we detected robust increases in GCaMP fluorescence in TN-derived filopodia during early stages that were characterized by high motility (Fig. 2B). We also observed episodic GCaMP signals in stabilized ectopic contacts made onto the VL muscles (Fig. 2C). The presence of episodic Ca^{2+} signals within the developing contacts is consistent with the roles that motoneuronal $Ca(v)2.1$ and $Ca(v)3$ channels play in synaptic refinement (see below), as well as the fact that embryonic ectopic contacts that remain in place will develop into functional synapses (Chang and Keshishian, 1996; Carrillo et al., 2010).

Calcium oscillations develop during NMJ maturation

During late stages of embryogenesis, Ca^{2+} transients at the developing NMJs became progressively more regular and frequent. GCaMP imaging at 18.5 h AEL revealed a single Ca^{2+} transient event every 2 min (0.0083 Hz; Fig. 3C,D), increasing to 1 event/min at 19.5 h AEL (0.016 Hz; Fig. 3C,E), and finally 2 events/min during the final 3 h of embryogenesis (0.033 Hz; 20–23 h AEL; Fig. 3C,F,G). Although the frequency of Ca^{2+} events remained constant during the final 3 h of embryogenesis, the patterning became regular by 21 h AEL (Fig. 3G). Tested using Fourier transform analysis software, by 21 h AEL, >40% of the embryos demonstrated regular and stable Ca^{2+} oscillations, with a mean frequency of 0.033 Hz.

Presynaptic $Ca(v)2.1$ and $Ca(v)3$ calcium channels are required for synaptic refinement

As Ca^{2+} signals were detected at both ectopic and native motoneuron terminals during the critical period for synaptic refinement, we tested the effect of knocking-down Ca^{2+} channels on synaptic connectivity and development. In separate experiments, RNAi constructs were expressed pan-neurally during embryonic and larval development to target each of the known genes that encode α subunits of voltage-gated Ca^{2+} channels (VGCCs): the $Ca(v)1$ channel gene *Dmca1D*, the $Ca(v)2.1$ gene *cacophony* (also known as *Dmca1A*), and $Ca(v)3$ gene *Dmca1G* (Fig. 4). Compared with control larvae, animals expressing RNAi-knockdowns of either *cacophony* or *Dmca1G* had an elevated frequency of ectopic contacts (Fig. 4G). By contrast, RNAi-knockdown of *Dmca1D* did not have a miswiring phenotype, although Dmca1D-RNAi has been shown to reduce Ca^{2+} currents in *Drosophila* larval motoneurons (Worrell and Levine, 2008). An elevated ectopic frequency was also observed in larvae expressing the RNAi construct for the auxiliary Ca^{2+} channel β subunit that is required for channel function (Catterall, 2011; Kanamori et al., 2013).

We next examined larvae bearing viable genetic mutations for *cacophony* and *Dmca1G*, to determine whether they would exhibit a miswiring phenotype similar to that observed in the above RNAi-knockdown experiments. We tested two hypomorphic *cac* alleles, cac^{NT27} and cac^{TS3} (Rieckhof et al., 2003). Larvae homozygous for either allele have an elevated frequency of ectopic contacts compared with WT (Fig. 4H). The ectopic frequency in cac^{NT27} homozygotes was higher than cac^{TS3} homozygotes, consistent with their phenotypic severity, as previously characterized (Rieckhof et al., 2003). Similarly, $Dmca1G^{null}$ homozygotes (Ryglewski et al., 2012) have a higher frequency of ectopic contacts
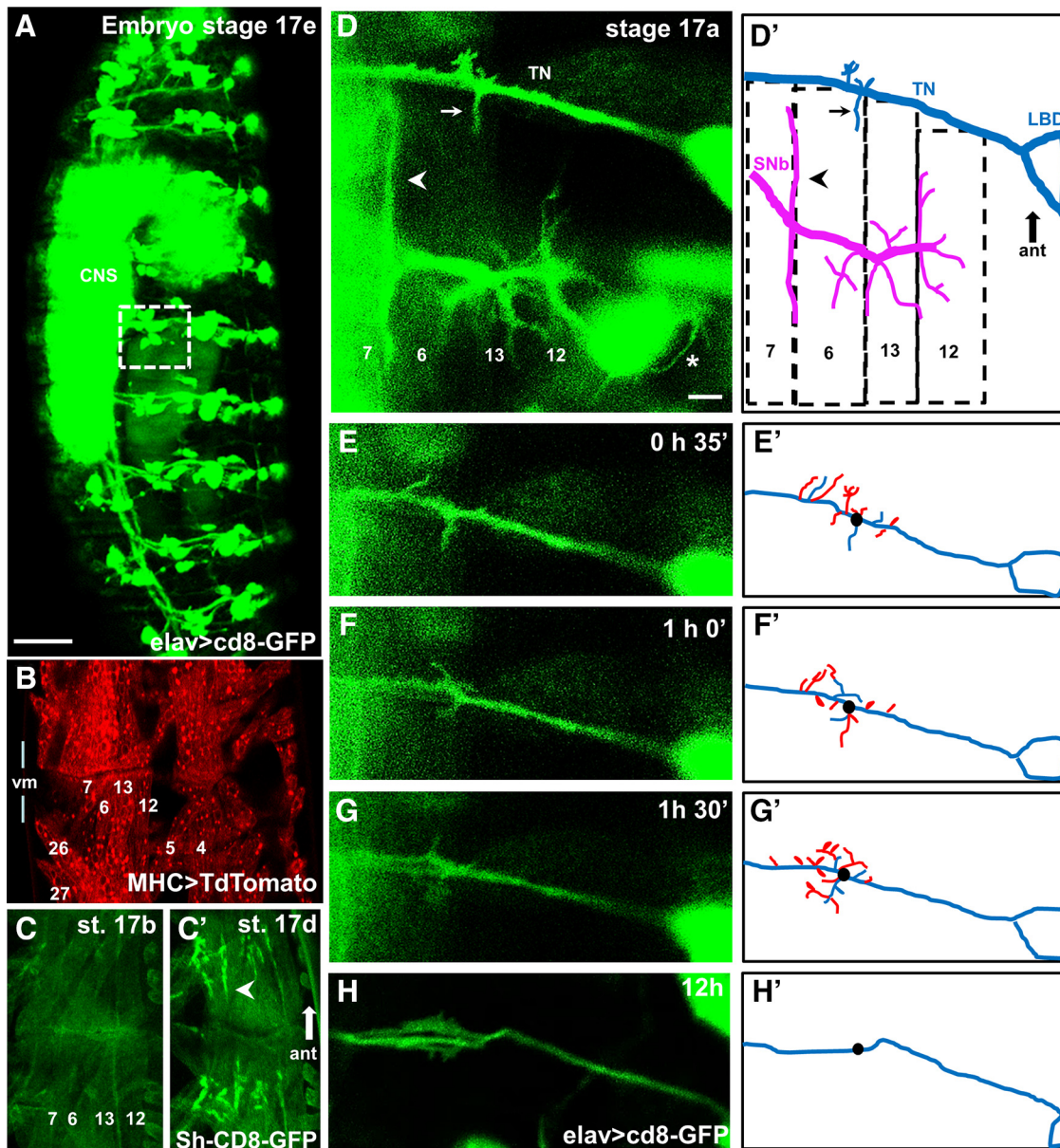
Figure 1. Live imaging of growth cones reveals that filopodia repeatedly contact off-target muscles during the last hours of embryogenesis. **A**, Pan-neural CD8-GFP expression in a Stage 17e *Mhc1* mutant embryo (21 h AEL) shows unaffected nervous system development. The presence of all peripheral nerves, sensory cells, as well as a condensed CNS is evident. White square represents the area shown in **D** that includes the TN and the SNb nerve innervating the internal VL muscles 7, 6, 12, and 13 in the abdominal segment A3. Scale bar, 50 μm. **B**, Two adjacent hemisegments in an intact *Mhc1* embryo expressing CD8-mCherry using the pan-muscular driver MHC-GAL4, revealing the presence of all body wall muscles. For orientation, the relative position of muscles 4, 5, 6, 7, 12, 13, 26, and 27 is labeled. **C**, The development of postsynaptic sites in *Mhc1* embryos appears unaltered, as postsynaptic GFP-tagged potassium Shaker channels (MHC-Sh-CD8-GFP) transition from a dispersed (Stage 17b, 17 h AEL, **C**) to a restricted (Stage 17d, 20 h AEL, **C'**) localization in bouton-like structures (arrowhead) during embryogenesis. Muscles 6, 7, 12, and 13 are labeled for orientation. **D**, Motoneuron filopodia from growth cones on the TN and SNb nerve in a Stage 17a *Mhc1* embryo (16.5 h AEL) as revealed by pan-neural GFP expression with a corresponding schematic showing the relative positions of muscles 6, 7, 12, and 13. Filopodial contacts simultaneously form on muscle 6 from correct (arrowhead) and incorrect (arrow) synaptic partners. Cell bodies from multiple sensory cells, including LBD that is part of the TN, are also fluorescent. The growth of sensory dendritic filopodia is evident (asterisk). Scale bar, 5 μm. **E–H**, Time-lapse snapshots of the TN in the same intact embryo at different time points, defining the image shown in **D** as the starting point. To illustrate filopodial dynamism, the corresponding schematics (**E'–H'**) depict filopodia extending off the TN at the time of the snapshot (blue) as well as filopodia that retracted 30 min before the snapshot (red). As reference, the black dot represents the origin of a prominent branch at time 0 shown in **D**.

compared to controls. We imaged Ca^{2+} signals in *cac^{NT27}* and *Dmca1G^{null}* mutant embryos to evaluate the frequency and pattern of Ca^{2+} signals in developing motoneuron terminals, and found that the frequency was significantly lowered in both the *cac^{NT27}* and *Dmca1G^{null}* mutants (Fig. 4I). These results provide evidence that presynaptic Ca^{2+} influx via VGCCs is essential for the removal of neuromuscular ectopic contacts and that, in either mutant, the frequency of Ca^{2+} transients in embryonic NMJs is reduced.

The calcium-dependent phosphatase CaN is required presynaptically for the removal of ectopically located neuromuscular contacts

Given the evidence for episodic Ca^{2+} influx in growth cones during the exploration of both off-target and on-target muscles, we next examined the downstream effectors involved in synaptic refinement. Our previous studies have implicated a role for both CaMKII (Carrillo et al., 2010) and the Ca^{2+}-dependent adenylyl
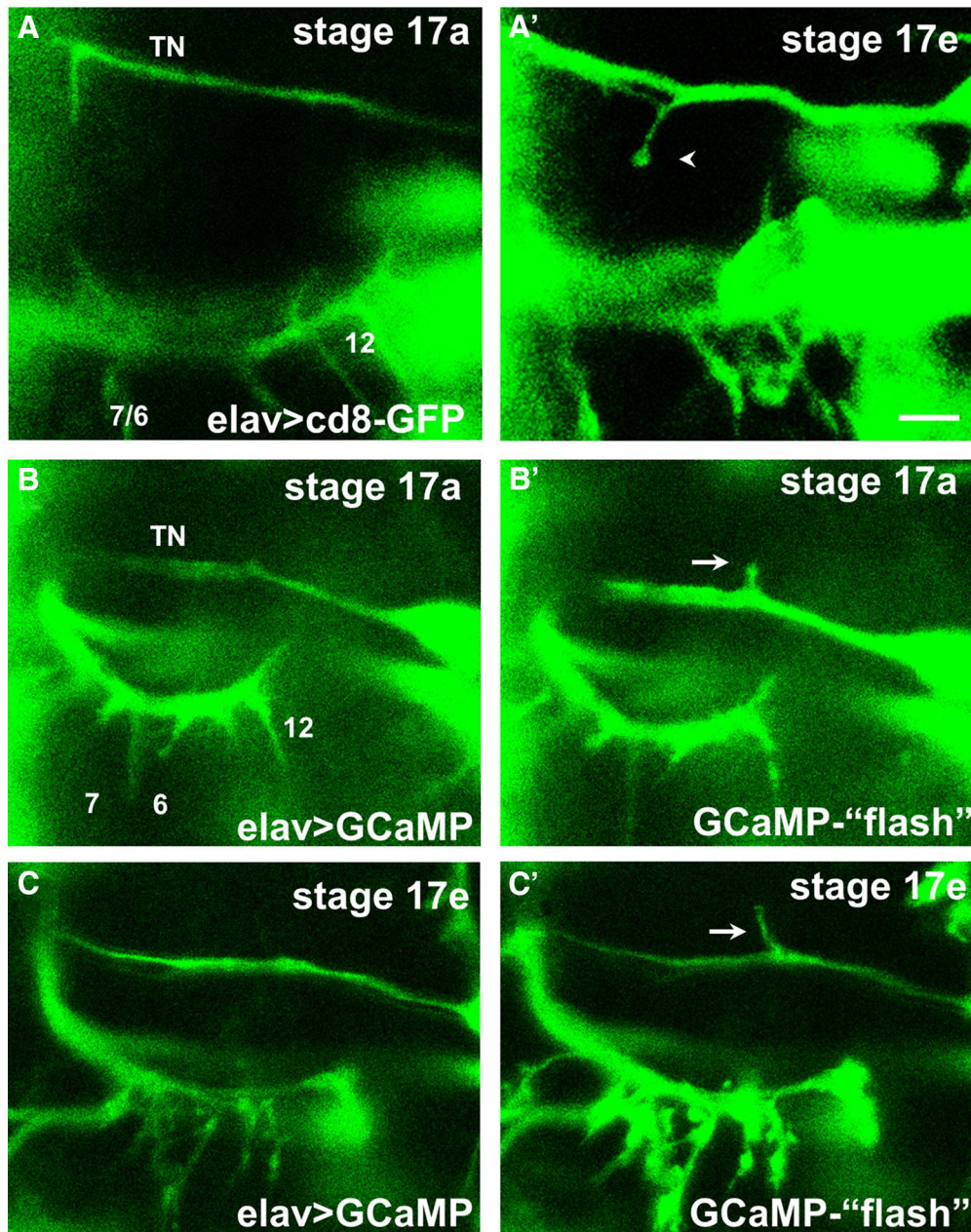
Figure 2. *In vivo* imaging of ectopic contacts during embryogenesis reveals the formation of bouton-like structures and intracellular Ca^{2+} signals. *A*, *A'*, Time-lapse images of the formation of an ectopic contact on muscle 6 in an intact embryo expressing CD8-GFP pan-neurally. At early stages (Stage 17a, ~16.5 h AEL, *A*), a prominent filopodium formed from the TN. Several hours later (Stage 17e, *A'*), motile filopodia are no longer observed, and an ectopic branch on muscle 6 that failed to retract showed bouton-like morphology (arrow). Scale bar, 5 μm. *B*, *C*, Motoneuron filopodia and terminals from the TN and SNb nerves at two different stages in the same animal. Changes of intracellular Ca^{2+} are revealed by increases in GCaMP fluorescence ("flashes," *B'*, *C'*) compared with the basal fluorescence (*B*, *C*). Ca^{2+} signals are observed in ectopic filopodia branching off the TN (arrows) at early (*B'*) stages of embryogenesis when most motoneuron growth cones are motile, as well as at late stages (8 h later, *C'*) when native SNb terminals showed bouton-like structures.

cyclase (Vonhoff and Keshishian, 2017a) in regulating synaptic refinement at the *Drosophila* NMJ. A third candidate for acting downstream of Ca^{2+} entry is the Ca^{2+}-dependent protein phosphatase CaN. CaN is involved in growth cone motility and turning behavior (Ferreira et al., 1993; Chang et al., 1995; Lautermilch and Spitzer, 2000; Wen et al., 2004), but its role in synapse formation and refinement *in vivo* is not as well defined.

CaN is a heterodimeric Ca^{2+}/calmodulin-dependent serine/threonine protein phosphatase composed of a catalytic subunit, CanA, and a regulatory subunit, CanB (Klee et al., 1979). In *Drosophila*, three genes encode distinct isoforms of CanA subunits (CanA-14F, CanA-14D, and CanA1), whereas two isoforms of

CanB subunits are encoded by the genes CanB and CanB2 (Takeo et al., 2006). We tested a role of CaN in synaptic refinement by expressing RNAi constructs pan-neurally for all three CanA genes as well as the two CanB genes in separate experiments. This was done in the presence of a Dicer2 transgene that effectively enhances the RNAi knockdown of CaN genes (Tomita et al., 2011). RNAi knockdown of each of the three CanA genes or CanB led to an elevated frequency of ectopic contacts compared with controls (Fig. 5D). Knockdown of CanB2 showed a small but not significant increase in ectopic contact frequency (Fig. 5D).

We tested whether animals bearing mutations in each of the CanA genes would match the miswiring phenotype observed
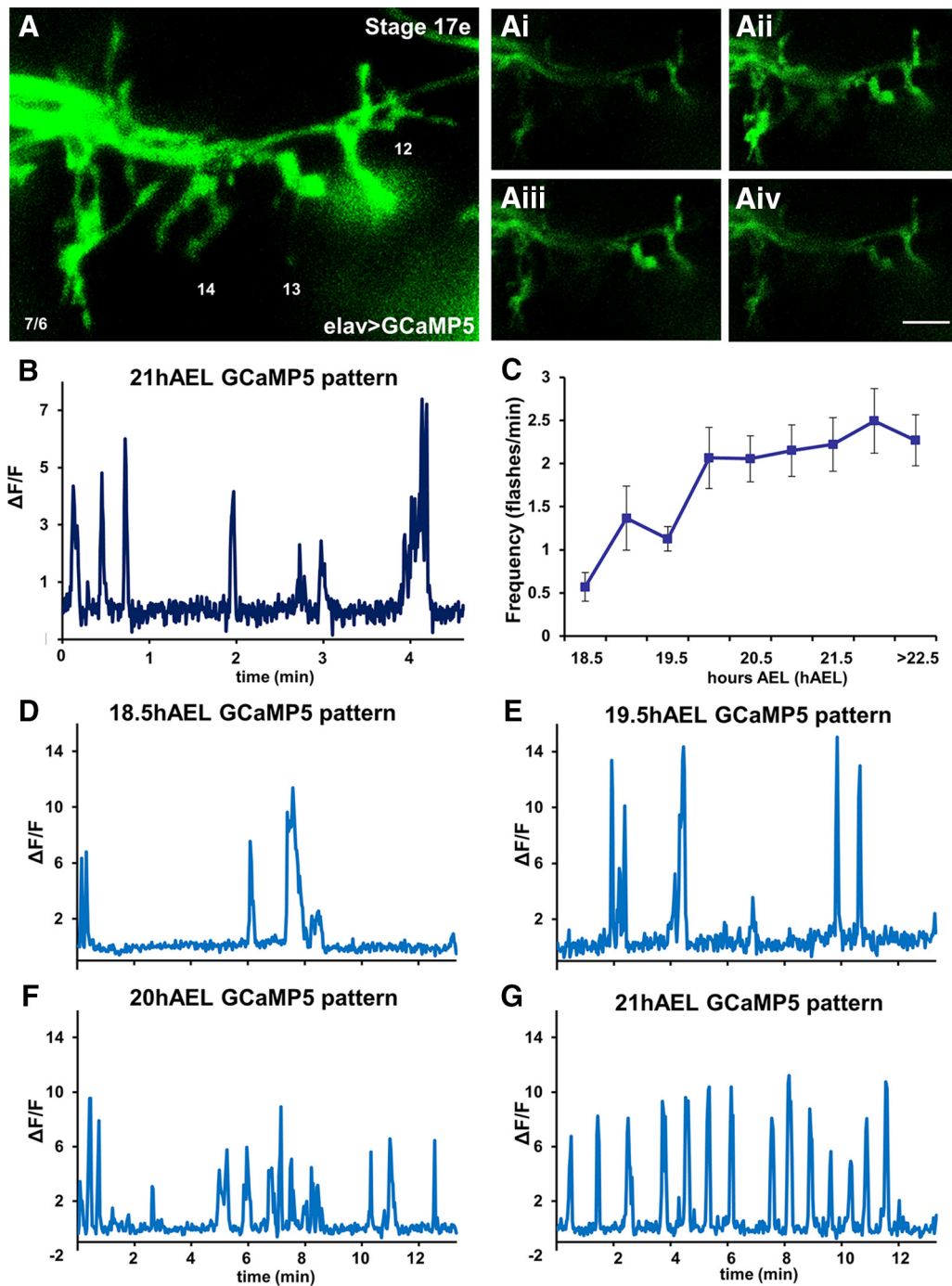
Figure 3. Low-frequency Ca^{2+} oscillations are observed at single motoneuron terminals in late embryogenesis. **A**, Motoneuron terminals from the SNb nerve in segment A3 of a Stage 17e embryo as revealed by the basal GCaMP fluorescence imaged with enhanced acquisition parameters to better visualize anatomy. **Ai–Aiv**, Dynamic changes in intracellular Ca^{2+} are quantified at the single-cell level by comparing basal GCaMP fluorescence (**Ai**, **Aiv**) with increased fluorescent levels (**Aii**, **Aiii**). Scale bars: **A**, 5 μm; **Ai–Aiv**, 10 μm. **B**, Example of changes in intracellular Ca^{2+} in boutons of a single motoneuron, RP3, as measured by changes in GCaMP basal fluorescence (ΔF/F) imaged every 300 ms (2 Hz). The pattern reveals that activity events last for several seconds before GCaMP fluorescence returns to baseline. **C**, Frequency of GCaMP flashes at different developmental stages. A twofold increase in the intracellular Ca^{2+} events was observed between Stages 17c-d (18.5–19.5 h AEL) and the last embryonic Stage 17e (20 h AEL), reaching an average frequency of 2 events/min during the last hours of embryonic development ($n = 7, 10, 14, 10, 8, 14, 7, 10,$ and 8, respectively). **D–G**, Examples of GCaMP patterns at different developmental stages measured at a single motoneuron, RP3, imaged every 2 s (0.5 Hz). Ca^{2+} signals progress from variable activity patterns (**D–F**) to a coordinated oscillatory pattern as observed in late embryos (**G**).

with expression of the RNAi constructs. Indeed, an elevated frequency of ectopic contacts was observed in mutant larvae homozygous for each of the three CanA genes (Fig. 5E). A high frequency of ectopic contacts was also observed in *CanA-14D/+* heterozygotes (Fig. 5E). The genetic specificity of the miswiring phenotype was confirmed by examining animals bearing chromosomal deficiencies that spanned the CanA gene loci (data not shown). To further confirm the presynaptic role of CanA for synaptic refinement, we expressed WT CanA14D either in all neurons or all muscles in *CanA-14D/+* heterozygotes. A significant rescue of the miswiring phenotype was observed only with the pan-neural expression of WT CanA14D (Fig. 5F). No rescue

was observed by the pan-neural expression of a catalytically inactive mutant form of CanA14D, containing an amino acid substitution at His217 to glutamine (CanA14D-H217Q) (Takeo et al., 2012), suggesting that phosphatase activity is required for the removal of ectopic contacts.

To test whether elevated CaN function would similarly disrupt synaptic refinement, we expressed pan-neurally three different constructs: CanA14D-WT, as well as a constitutively active form of CanA14D (CanA14D^{act}) and CanA-14F (CanA14F^{act}) as separate gain-of-function (GOF) experiments (Sullivan and Rubin, 2002; Nakai et al., 2011). In contrast to the above loss-of-function (LOF) experiments, no increased frequency of ectopic contacts was observed (Fig. 5E).

The molecular pathway underlying synaptic refinement involves Ca^{2+}-dependent signaling involving CaN, PKA, and protein phosphatase-1 (PP1) function

We next performed genetic interaction tests to determine whether a functional relationship existed between CaN and any of the genes previously described as being

←

and 17. On muscles 7 and 6, the ectopic contacts (red, arrows) are shown in the typical locations in which they are observed next to the native stereotypic motoneuron contacts (arrowhead). Blue represents TN. Green represents segmental nerve b (SNb). Gray represents segmental nerve d (SNd). Blue dashed square represents the area shown in images of ectopic contacts in Figures 4, 5, and 7. **B–F**, Ectopic contacts on muscles 7 and 6 were detected in third instar larvae in genetic manipulations that affect voltage-gated Ca^{2+} channels. Ectopic contacts comprised all different bouton types, ranging from ectopic Type 1b endings emerging from the TN (**D**) or from motoneurons innervating neighboring muscles (**E**), as well as Type II endings (**C**, **F**). **C–F**, Arrow indicates ectopic contact. Arrowhead indicates native innervation. Scale bars: **B**, **D**, **F**, 40 μm; **C**, 25 μm; **E**, 15 μm. **G**, Frequency of ectopic contacts in larvae expressing RNAi constructs for all genes encoding for α subunits of voltage-gated Ca^{2+} channels, cacophony (cac, Ca(v)2.1), Dmca1D (Ca(v)1), and Dmca1G (Ca(v)3), as well as for the Ca^{2+} channel β subunit, using the pan-neural elavGAL4^{C155} driver. Control groups included elavGAL4 flies crossed to either W1118 or UAS-GFP flies, and experimental lines were compared with their corresponding control for statistical significance. Data are calculated as the percentage of ectopic-containing hemisegments per larva, averaged over the number of animals (±SEM; n = 19, 12, 22, 8, 26, and 18 animals, respectively; p = 0.005, 0.006, and 0.008, respectively). **H**, Frequency of ectopic contacts in WT and homozygous and heterozygous larvae for cac^{NT27}, cac^{TS3}, and Dmca1G (n = 51, 36, 61, 17, 10, 34, and 18 animals, respectively; p = 1.1×10^{-18}, 8.8×10^{-8}, 0.01, and 1.1×10^{-6}, respectively). **I**, Frequency of GCaMP5 flashes in Stage 17e embryos in control, cac^{NT27}, and Dmca1G homozygotes, measured at a single motoneuron as described in Figure 3 (n = 21, 13, and 13, respectively; p = 0.0004 and 0.009, respectively).
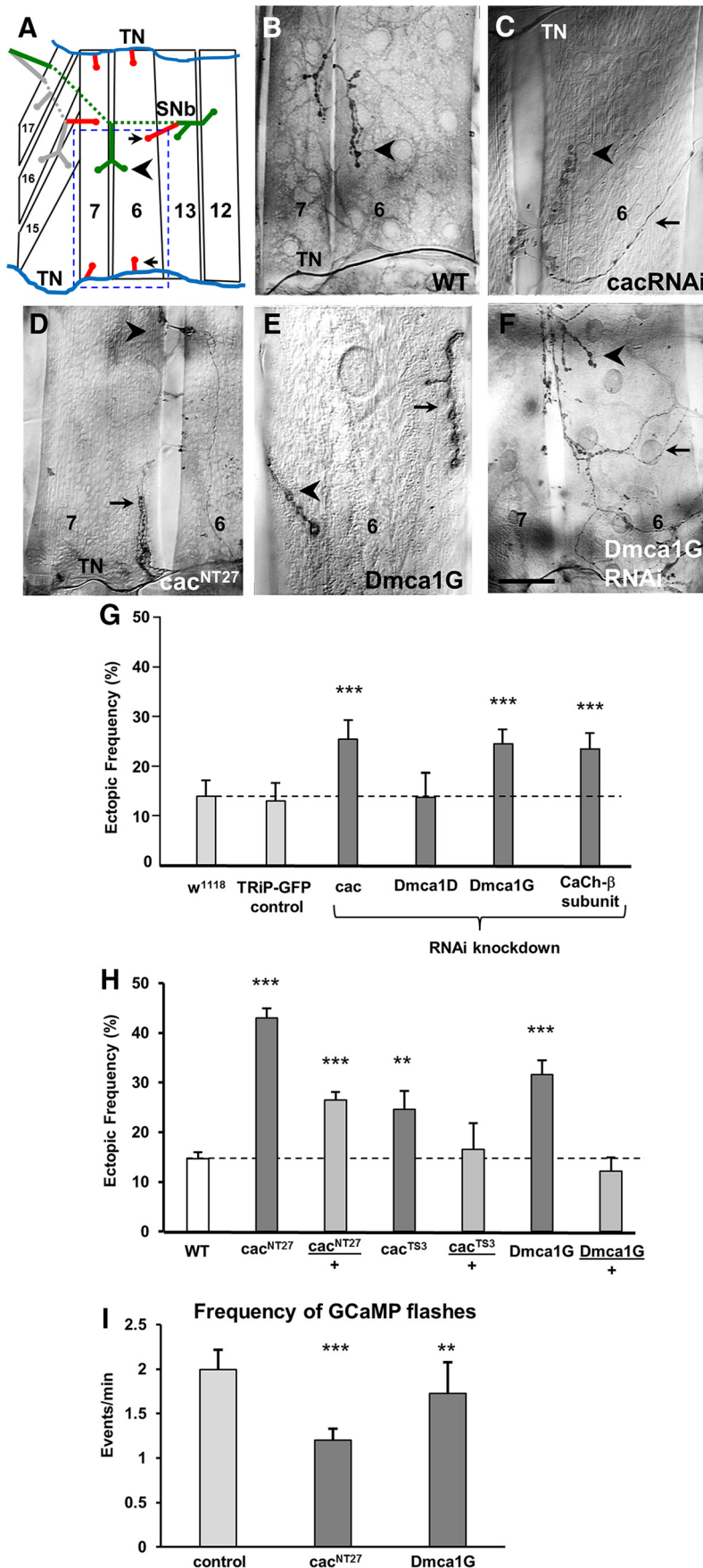
Figure 4. LOF of the voltage-gated Ca(v)2.1 *cacophony* and Ca(v)3 *Dmca1G* Ca channels leads to miswiring. **A**, Schematic of the musculature of the ventral portion of one abdominal hemisegment of a third instar larva showing muscle fibers 6, 7, 12, 13, 15, 16,

required for refinement. We first tested the interaction between CanA and the Ca^{2+} channel gene *cacophony*, using $cac^{NT27}/+$ heterozygotes that show elevated ectopic contact frequency. A suppression of the phenotype was observed in all double heterozygotes of CanA and cac^{NT27} (Fig. 6A). The ectopic contact frequency observed in $cac^{NT27}/+$ animals was significantly lower in the double heterozygote $cac^{NT27},+/+,CanA14F$ as well as in $cac^{NT27}/+;;CanA1/+$. Similarly, $cac^{NT27},+/+,CanA14D$ heterozygotes showed a suppressed ectopic frequency compared with $CanA14D/+$ mutants (Fig. 6A).

We previously showed that refinement required components of a cAMP-dependent pathway, including the adenylyl cyclase Rutabaga, the cAMP-phosphodiesterase Dunce, PKA, and PP1 (Vonhoff and Keshishian, 2017a). Therefore, we investigated whether CanA interacts genetically with any of these molecules. We tested for a suppression of the ectopic contact phenotype observed in $CanA14D/+$ heterozygotes, by crossing $CanA14D$ females to males mutant for *rutabaga* (rut^1), *dunce* (dnc^{M11}), PKA subunit-R2 ($PKAR2^{LOF}$), and protein phosphatase-1 ($PP1a96A$). Similar ectopic frequencies in the double heterozygotes $CanA14D, +/+, rut^1$ and $CanA14D, +/+, dnc^{M11}$ were observed compared with $CanA14D/+$ animals (Fig. 6B). By contrast, a significant reduction of the $CanA14D/+$ phenotype was observed in $CanA14D/+; PKAR2^{LOF}/+$ and $CanA14D/+;;PP1a96A/+$ double heterozygotes (Fig. 6B). These results suggest that CaN, PKA, and PP1 may function in the same signaling pathway underlying refinement.

In mammalian neurons PKA phosphorylates protein inhibitor-1 (I1+), which in turn inhibits PP1. By contrast, CaN dephosphorylates I1+, activating PP1 (Oliver and Shenolikar, 1998). Thus, we hypothesized that CaN and PKA may also regulate common targets in opposite ways, although their interactions in *Drosophila* are less well understood, and I1+ has as yet no known fly homolog (Ceulemans et
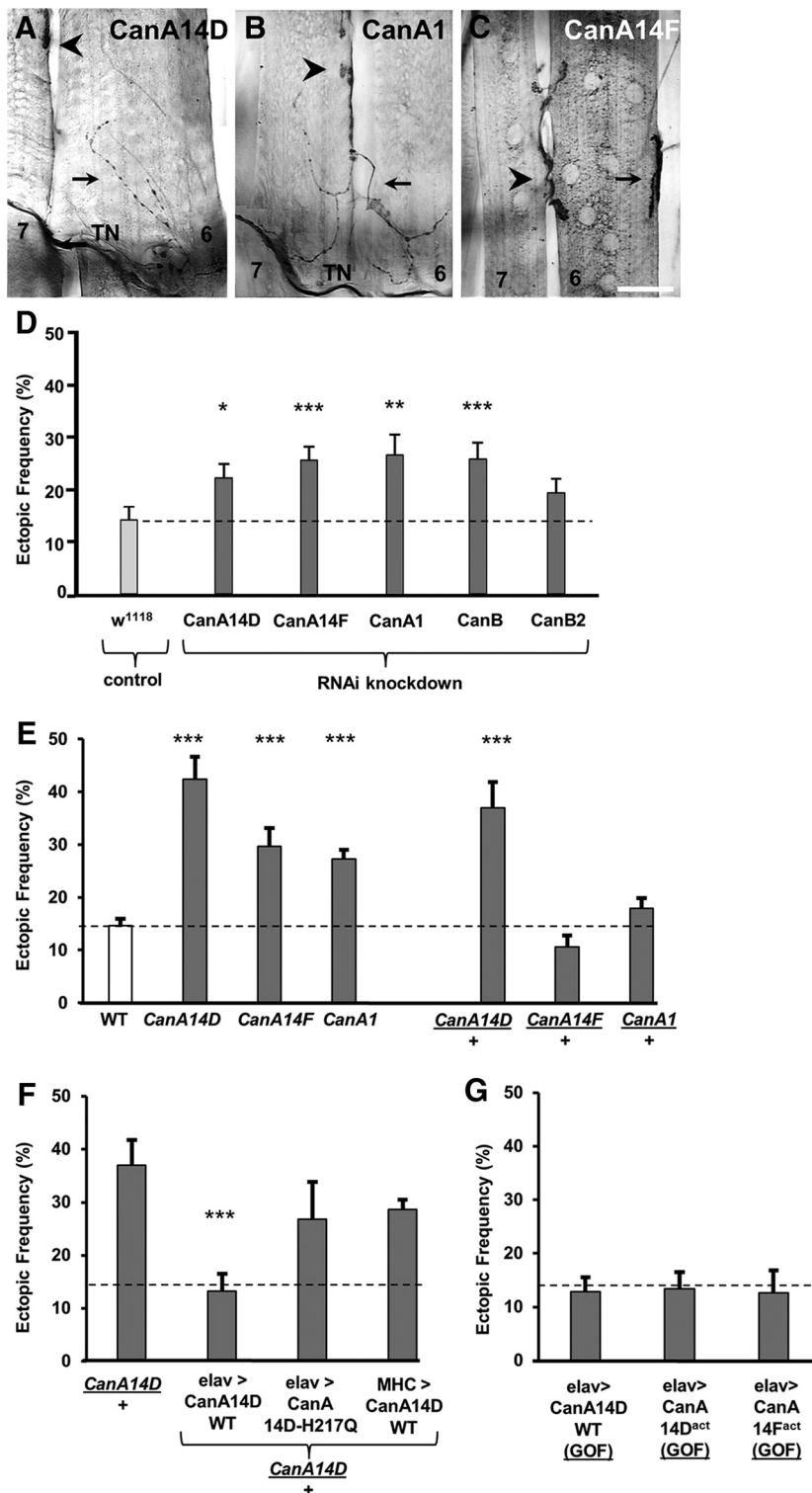
←

Figure 5. The Ca^{2+}-dependent phosphatase CaN is required presynaptically for refinement. *A–C*, The segmental border region of muscles 7 and 6 of a third instar larvae is shown from a mutant for each of the three genes encoding for a regulatory CaN subunit A (CanA) *CanA14F* (*A*), *CanA1* (*B*), and *CanA14D* (*C*). Arrow indicates ectopic contact. Arrowhead indicates native innervation. Scale bars: *A*, 25 μm; *B*, *C*, 40 μm. *D*, Frequency of ectopic-containing hemisegments in larvae expressing RNAi for the indicated CaN genes using the elav-GAL4 driver. The control group included elav-GAL4 flies crossed to W1118 (n = 19, 19, 21, 22, 26, and 16, respectively; p = 0.02, 0.005, 0.002, and 0.003, respectively). *E*, Ectopic frequency in WT (white), and *CanA14F*, *CanA1*, and *CanA14D* homozygotes and heterozygotes (dark gray) (n = 51, 18, 21, 15, 26, 20, and 25, respectively; p = 1.6 × 10^{-6}, 0.0002, 2.1 × 10^{-6}, and 8.7 × 10^{-5}, respectively). *F*, As a rescue experiment, the elevated ectopic frequency observed in *CanA14D/+* heterozygotes is reduced only by the pan-neural expression of a CanA14D WT transgene (*CanA14D/+;UAS-CanA14D-WT/+*; elavGS-GAL4,UAS-CD8-GFP/+). By contrast, no rescue was observed following the panmuscular expression of CanA14D WT (*CanA14D/+;UAS-CanA14D-WT/+;MHCGAL4,UAS-CD8-mCherry/+*) or the pan-neural expression of a catalytically inactive

mutant form of CanA14D, containing an amino acid substitution at His217 to glutamine (CanA14D-H217Q) (*CanA14D/+;* UAS-CanA14D-H217Q/+;elavGS-GAL4,UAS-CD8-GFP/+) (n = 21, 9, 10, and 18, respectively; p = 0.0002). *G*, GOF experiments involved the pan-neural expression of the CanA14D WT transgene (elav-GAL4/>;UAS-CanA14D-WT/+) or a constitutively active form of CanA14D (UAS-CanA14D^{act}/elavGS-GAL4,UAS-CD8-GFP), as well as CanA14F (elav-GAL4/+;UAS-CanA14D-WT/+). No effects on connectivity were observed in these manipulations (n = 18, 12, and 8, respectively). *p < 0.05. **p < 0.01. ***p < 0.001.
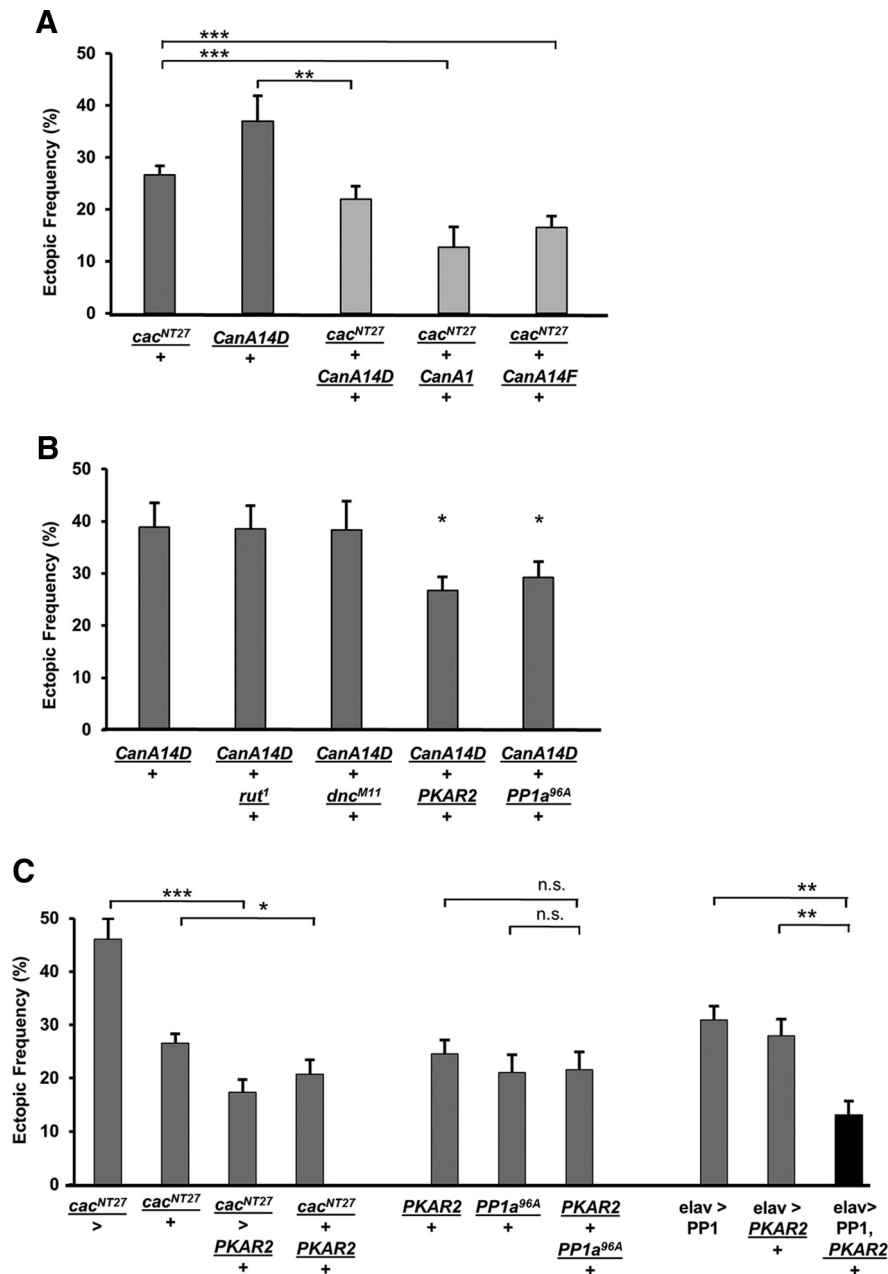
Figure 6. Genetic interaction tests indicate that CanA may function in a pathway that involves Ca^{2+} signaling, PKA, and PP1 function for refinement. **A**, The ectopic frequency observed in $cac^{NT27}/+$ heterozygotes was reduced in genetic backgrounds heterozygous for CanA mutations ($n = 54, 21, 29, 13$, and 29, respectively; $p = 0.003, 0.004$, and 0.002, respectively). **B**, The elevated ectopic frequency observed in $CanA14F/+$ heterozygotes was reduced in mutant backgrounds that affect PKA and PP1 function ($n = 20, 8, 12, 23$, and 21, respectively; $p = 0.02$ and 0.04, respectively). **C**, A genetic background for increased PKA function suppresses the elevated ectopic frequency observed in $cac^{NT27}/+$ heterozygotes and in larvae overexpressing PP1 pan-neurally ($n = 12, 54, 19, 20, 10, 18, 12, 18$, and 22, respectively; $p = 9.9 \times 10^{-6}, 0.04, 0.0004$, and 8.2×10^{-6}). *$p < 0.05$. **$p < 0.01$. ***$p < 0.001$.

al., 2002; Bennett et al., 2006). We reasoned that increased PKA function would cause phenotypes similar to those seen with decreased CaN function. Therefore, we used $PKAR2^{LOF}$ mutants that have elevated PKA activity due to mutations in the regulatory subunit R2 (Park et al., 2000), and crossed them to cac^{NT27} mutants. Consistent with our hypothesis, a rescue of the miswiring phenotype was observed in $cac^{NT27}/>$; $PKAR2^{LOF}/+$ hemizygous males and $cac^{NT27}/+$; $PKAR2^{LOF}/+$ heterozygous females (Fig. 6C). Although PKA and PP1 functions were previously described as being required for refinement, their functional interaction within

the signaling pathway remained untested. Therefore, we hypothesized that the ectopic contact phenotype observed in $PKAR2^{LOF}$ mutants may be caused by an elevated inhibition of PP1, similar to the phenotype observed in $PP1a96A$ mutants. Testing this, we observed a suppression of the miswiring phenotype by the pan-neural expression of PP1 in $PKAR2^{LOF}$ mutants, whereas no rescue was observed in the $PKAR2^{LOF}/+$; $PP1a96A/+$ double heterozygotes (Fig. 6C). These results suggest that CaN, PKA, and PP1 likely function together, downstream of Ca^{2+} influx, to mediate off-target contact removal.

Misregulation of CaMKII function results in miswiring

How might CaN, PKA, and PP1 collectively regulate the removal of ectopic contacts during synaptic refinement? A previous study showed that presynaptic CaMKII function is essential for synaptic refinement at the *Drosophila* NMJ (Carrillo et al., 2010). In mammalian cells, CaMKII function is regulated by both CaN and PP1 activity (Shields et al., 1985; Oliver and Shenolikar, 1998). The interaction between these molecules in *Drosophila* is less well understood, and whether they act in the same signaling pathway for refinement remains an open question. Therefore, we performed genetic interaction tests to examine whether the ectopic phenotype observed in $CanA14D/+$ heterozygotes is rescued by CaMKII mutations. An elevated ectopic contact frequency was observed in $CanA14D/+$;;; $CaMKII/+$ double heterozygotes (Fig. 7D). This indicates that reduced CaMKII-dependent phosphorylation does not compensate for reduced CaN function. Whereas the miswiring phenotype observed in cac^{NT27} mutants was rescued by lowering CaN function (Fig. 6), reduced CaMKII function in cac^{NT27} mutants did not rescue the miswiring phenotype, given the elevated ectopic contact frequency observed in $cac^{NT27}/+$;;;$CaMKII/+$ double heterozygotes (Fig. 7D). These results support the view that CaMKII function is critical for synaptic refinement. Therefore, we sought to further examine the role of CaMKII in the removal of ectopic contacts.

We first examined the phenotype of both LOF and GOF of CaMKII in motoneurons (Fig. 7E). Four different CaMKII constructs were examined: (1) the inhibitory transgene CaMKII-Ntide; (2) the mutated form CaMKII-T287A, which has normal Ca^{2+}-dependent activity but blocked autophosphorylation; (3) the mutated form CaMKII-T287D, which is constitutively active and Ca^{2+}-independent; and (4) the WT form CaMKII-R3 (Fig. 7E). A significant elevated ectopic frequency was observed
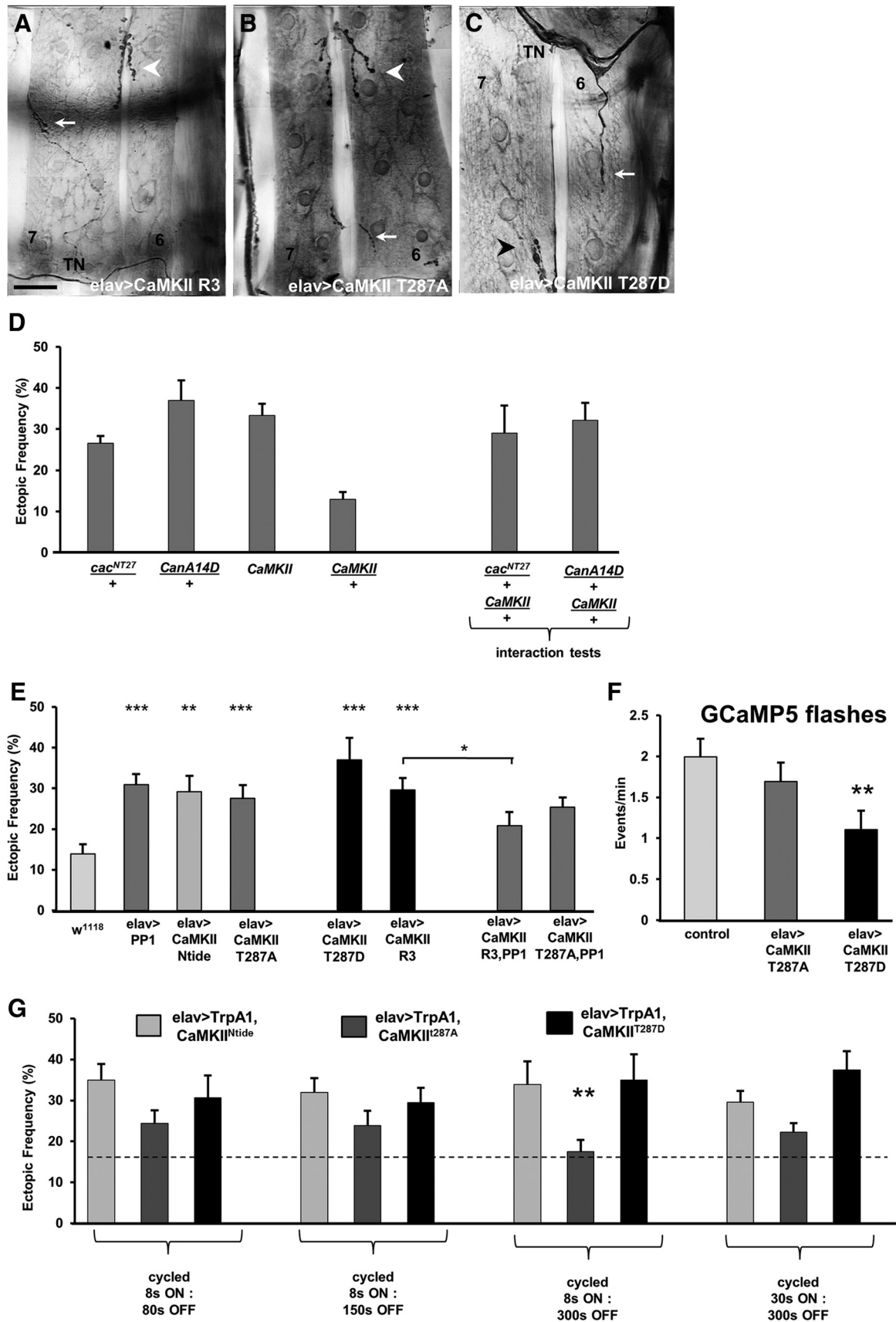
Figure 7. Misregulation of CaMKII function affects synaptic refinement in a pathway that likely involves Ca^{2+} signaling and PP1. **A–C**, Ectopic contacts on muscles 7 and 6 are shown in larvae expressing a WT CaMKII form (CaMKII-R3, **A**), a Ca^{2+}-dependent mutant CaMKII T287A (**B**), and a constitutively active CaMKII form (CaMKII T287D, **C**). Arrow indicates ectopic contact. Arrowhead indicates native innervation. Scale bars: **A**, **B**, 40 μm; **C**, 25 μm. **D**, The elevated ectopic frequency observed in cac^{NT27}/+ and $CanA14D$/+ heterozygotes was not suppressed in $CaMKII$ heterozygous mutants (n = 54, 20, 19, 18, 6, and 19, respectively). **E**, Elevated ectopic frequency was observed in larvae expressing genetic constructs that increase and (*Figure legend continues.*)

in larvae with loss of CaMKII function as well as when autophosphorylation was blocked. Similarly, overexpression of either the WT R3 form or the constitutively active T287D transgene both showed a significantly elevated ectopic contact phenotype.

CaMKII is inhibited by PP1-dependent dephosphorylation in mammalian cells (Shields et al., 1985). Therefore, we tested whether a similar relationship occurred in *Drosophila*, and hypothesized that elevated CaMKII activity would be balanced by increased PP1 function. Indeed, the high frequency of ectopic contacts observed in larvae overexpressing the WT CaMKII-R3 form was significantly reduced by coexpression of PP1 (Fig. 7E). As expected, no rescue of the phenotype was observed in animals coexpressing the autophosphorylation LOF CaMKIIT287A and PP1 (Fig. 7E).

These results indicate that CaMKII is a key component of the molecular pathway underlying refinement, and that several molecules work together for its regulation. Why does increased as well as decreased CaMKII function negatively affect refinement? One hypothesis involves the possibility of an optimal range for CaMKII activity, where deviations in either direction would cause a phenotype. This would be similar to the situation observed elsewhere for several cAMP-dependent functions, such as reduced memory performance (Tully and Quinn, 1985), satellite bouton formation (Lee and Wu, 2010), sensory neuron dendrite complexity (Copf, 2014), and ectopic contact removal (Vonhoff and Keshishian, 2017a). However, we hypothesized that the CaMKII-GOF phenotype may be due to reduced neural excitability, as observed in larval motoneurons expressing the constitutively active form CaMKII-T287D (Park et al., 2002).

To test whether there is a loss of excitability in embryonic neurons, we live-imaged Ca^{2+} transients in motoneuron terminals of embryos expressing either the GOF CaMKII-T287D or the autophosphorylation mutant CaMKII-T287A. The frequency of Ca^{2+} transients was significantly reduced in embryos expressing the GOF-T287D form. By contrast, the frequency of Ca^{2+} events in embryos expressing the LOF-T287A did not differ from controls. This implies that the miswiring observed in the GOF T287D animals may be due to the reduced Ca^{2+} transient frequency, which would place CaMKII function upstream of Ca^{2+} signaling in the molecular pathway. Therefore, we further tested whether the miswiring phenotype observed in T287D animals was due to reduced Ca^{2+} influx or, alternatively, to abnormal regulation of CaMKII function. For this, we coexpressed the temperature-sensitive, Ca^{2+}-permeable cation channel TrpA1 (Hamada et al., 2008; Pulver et al., 2009) together with the T287D construct, and activated it at different frequencies by using a variety of temperature-shift protocols, providing another source of Ca^{2+} influx in addition to the native Ca^{2+} oscillation regulated by the central pattern generator (Fig. 3). No rescue of the miswiring phenotype was observed in T287D animals stimulated with any of the activation patterns, which included 1:10 duty cycles (8 s of

activation at 28°C [8 s ON] followed by 80 s of inactivation at 18°C [80 s OFF], as well as 30 s ON: 300 s OFF, Fig. 7G; and 15 s ON: 150 s OFF; data not shown), 1:20 and 1:40 duty cycles (8 s ON: 150 s OFF, and 8 s ON: 300 s OFF, respectively; Fig. 7G). By contrast, introducing additional Ca^{2+}influx following the 8 s ON: 300 s OFF pattern was sufficient to rescue the miswiring observed in animals expressing the T287A isoform, which is activated by Ca^{2+} transients but has blocked autophosphorylation. No rescue was observed following activation patterns with increased frequencies or duty cycles.

This result suggests that the lack of autophosphorylation in the CaMKII-T287A animals can be compensated for by increasing the frequency of Ca^{2+} transients to maintain CaMKII function in an optimal level. Increasing Ca^{2+} transients at too high frequencies likely leads to CaMKII overactivation, a similar scenario seen in animals expressing the constitutively active form CaMKII-T287D. Furthermore, no rescue of the miswiring observed in animals expressing the inhibitory construct CaMKII-Ntide was accomplished following any of the activation patterns. These results suggest that overactivation of CaMKII affects ectopic removal by misregulation of molecular components of the signaling pathway downstream of Ca^{2+} influx in addition to reducing membrane excitability. This indicates a key role of CaMKII in the molecular pathway underlying ectopic removal, in which several molecules regulate CaMKII to maintain its function within an optimal range.

Dmca1G, CaN, and CaMKII may function in the same molecular pathway to regulate Sema2a-dependent chemorepulsion

Previous studies have shown that ectopic contact removal from off-target muscles depends on Sema2a, a chemorepellant secreted by the muscle that binds to its presynaptic receptor, PlexinB, to induce repulsion (Matthes et al., 1995; Winberg et al., 1998; Hu et al., 2001; Ayoob et al., 2004). The activity-dependent removal of ectopic contacts is proposed to occur by modulating the motoneuron's responsiveness to Sema2a-dependent chemorepulsion (Carrillo et al., 2010; Vonhoff and Keshishian, 2017a). Therefore, we performed genetic interaction tests to examine whether the molecular components identified above may function in the same molecular pathway as Sema2a. For this, we tested *Dmca1G/+*, *CanA14F/+*, and *CaMKII/+* heterozygotes that each show relatively normal connectivity similar to WT animals but provide a sensitized genetic background to test for interactions with *Sema2a* heterozygotes. A significant enhancement of the ectopic contact phenotype was observed in all double heterozygotes, suggesting genetic interactions between the tested genes (Fig. 8).

To further test a relationship between CanA and chemorepulsion, we asked whether the ectopic phenotype observed in *CanA14D* mutants could be rescued by the pan-neural overexpression of the Sema2a receptor, PlexinB (Ayoob et al., 2006). *CanA14D* mutants overexpressing PlexinB significantly reduced the ectopic frequency (Fig. 8A), suggesting that CanA acts upstream of chemorepulsion. By contrast, pan-neural overexpression of the Ca(v)2.1 gene *cacophony* showed no rescue of the *CanA14D* phenotype, suggesting that CanA acts downstream of Ca^{2+}, consistent with its known role as Ca^{2+}-dependent phosphatase.

Having observed that ectopic filopodia branching off the TN extended and retracted on VL muscles during the final hours of embryogenesis (Fig. 1), we next asked whether reduced chemorepulsion would affect the dynamics of ectopic TN filopodia. We expressed membrane-tagged fluorescent probes pan-neurally

←

(*Figure legend continued.*) decrease CaMKII function. Pan-neural overexpression of PP1 reduced the ectopic frequency observed in larvae expressing the CaMKII WT form R3, but not the Ca^{2+}-dependent form T287A ($n = 23, 19, 18, 18, 26, 15, 29, 17,$ and 29, respectively; $p = 1.5E-05, 0.001, 0.0009, 0.0005, 8.1 \times 10^{-5},$ and 0.03, respectively). **F**, The frequency of GCaMP5 flashes is significantly reduced in embryos expressing the constitutively active form CaMKIIT287D but not in embryos expressing CaMKIIT287A ($n = 27, 12,$ and 9, respectively; $p = 0.004$). **G**, The temperature-sensitive Ca^{2+}-permeable channel TrpA1 was coexpressed with different CaMKII constructs, and temperature was cycled in a PCR machine following different activation protocols during the critical period of refinement ($n = 8, 13, 18, 7, 10, 5, 17, 19, 13, 12, 19,$ and 10, respectively; $p = 0.008$). *$p < 0.05$. **$p < 0.01$. ***$p < 0.001$.
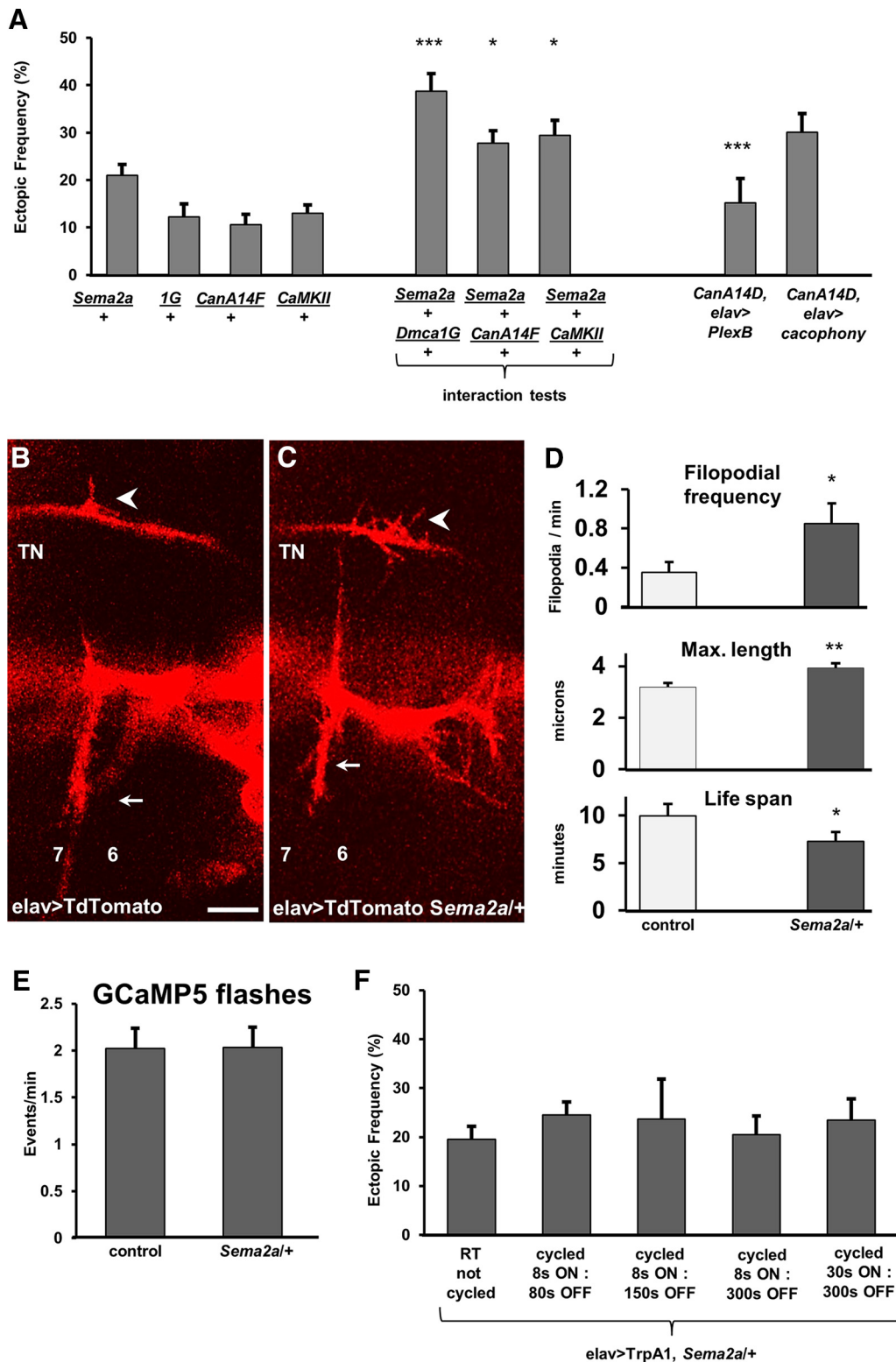
Figure 8. CanA and CaMKII may function in a pathway that involves Ca^{2+} signaling and Sema2a-dependent chemorepulsion for refinement. **A**, Genetic interactions were observed between heterozygous mutants for the trans-synaptic chemorepellant sema2a and heterozygotes for *Dmca1G*, *CanA14F*, and *CaMKII*. Rescue experiments by the pan-neural expression of PlexB (*CanA14D/>;;UAS-PlexinB/elavGS-GAL4,UAS-CD8-GFP*) or Cacophony (*CanA14D/+;;UAS-cacophony/elavGAL4,UAS-TdTomato*) in *CanA14D* mutants ($n = 34, 18, 25, 18, 17, 13, 27, 11,$ and 11, respectively; $p = 0.0002, 0.03, 0.02,$ and 0.0002, respectively). **B**, **C**, Motoneuron filopodia from growth cones on the TN and SNb nerve in a Stage 17a *Mhc1* embryo (16.5 h AEL) are shown as revealed by pan-neural TdTomato expression in a control animal (**B**) and a heterozygous *Sema2a* mutant (**C**). Arrow indicates ectopic filopodial contact. Arrowhead indicates native innervation. Muscles 7 and 6 are labeled for orientation. **D**, *In vivo* imaging of fluorescently tagged filopodia in intact embryos revealed that reduced Sema2a levels increased the frequency of ectopic filopodia branching off the TN (top: $n = 9$ and 6 embryos; $p = 0.03$) and maximum filopodial length (middle: $n = 110$ and 131 filopodia; $p = 0.001$), whereas it decreased the average filopodial life span (bottom: $n = 71$ and 51 filopodia; $p = 0.04$). Data are mean ± SEM. **E**, Frequency of GCaMP5 flashes recorded at a single RP3 bouton in 17e embryos in control and in *Sema2a* heterozygotes. **F**, Additional Ca^{2+} transients do not reduce ectopic frequency in *Sema2a/+* heterozygotes. The TrpA1 channels were expressed pan-neurally in Sema2a heterozygotes, and temperature was cycled in a PCR machine following different activation protocols ($n = 8, 13, 18, 7, 10, 5, 17, 19, 13, 12, 19,$ and 10, respectively). *$p < 0.05$. **$p < 0.01$. ***$p < 0.001$.

and analyzed morphological properties of ectopic TN filopodia in control and *Sema2a* heterozygous animals (Fig. 8B–D). We observed an increase in the frequency of TN filopodia as well as in the maximum filopodial length in *Sema2a* heterozygotes, whereas the average filopodial life span was decreased (Fig. 8D). To test whether Sema2a-dependent signaling acts downstream of presynaptic Ca^{2+}, we live-imaged Ca^{2+} signals in motoneuron terminals in *Sema2a/+* heterozygotes. Peristaltic activity as fictive motor waves was observed in Stage 17e *Sema2a/+* heterozygotes that was indistinguishable of the activity pattern observed in control embryos. At the single-cell level, a similar frequency of Ca^{2+} transients was observed in *Sema2a/+* heterozygotes and control animals (Fig. 8E). To further test that Ca^{2+} signaling may be positioned upstream of Sema2a signaling, we expressed the TrpA1 channel in *Sema2a/+* heterozygotes. Increased presynaptic Ca^{2+} influx did not reduce the ectopic frequency of *Sema2a/+* animals to WT levels in any of the TrpA1 activation protocols tested (Fig. 8F).

It should be noted that the genetic interaction tests of this study demonstrate functional relationships and do not necessarily imply direct physical interactions between the molecules. Although the simplest explanation is that the molecules participate in a common signaling pathway, it remains possible that multiple pathways are at play. Nevertheless, these genetic tests provide important evidence for unraveling the molecular mechanisms underlying synaptic refinement, and support our view that chemorepulsion plays a key role in the formation and refinement of off-target contacts *in vivo*. In summary, our results support the view that CaN, PKA, PP1, and CaMKII regulate the neuron's response to muscle-derived repulsion for the refinement of synaptic connectivity.

Discussion

We provide the first direct evidence for episodic Ca^{2+} signals at developing growth cones during the exploration of off-target and on-target synaptic partners at the *Drosophila* NMJ. Our results support a model in which presynaptic electrical activity and Ca^{2+} influx through VGCCs regulate the neuron's responsiveness to Sema2a-dependent chemorepulsion exerted by the muscle. Consistently, imaging of intact embryos demonstrated that decreased Sema2a levels promoted ectopic filopodial contacts and that Sema2a-dependent signaling may be acting downstream of presynaptic Ca^{2+} influx.

Calcium signals are observed during the formation and removal of ectopic contacts

Multiple *in vitro* studies have described a role for Ca^{2+} in regulating growth cone dynamics (Schubert et al., 1978). Ca^{2+} regulates the elongation and motility of filopodia and lamellipodia (Kater and Shibata, 1994; Rosenberg and Spitzer, 2011) and plays a role in chemotropic turning behavior (Gomez and Zheng, 2006; Zheng and Poo, 2007). However, the role of Ca^{2+} signaling during the innervation of correct and incorrect synaptic partners is not as well understood.

In *Drosophila* embryos, the silencing of electrical activity increases the appearance of inappropriate neuromuscular contacts that develop into functional synapses (Jarecki and Keshishian, 1995; White et al., 2001; Carrillo et al., 2010). Restoring electrical activity within an early critical period, spanning from late embryogenesis to the early first larval stage, rescues the miswiring phenotype (Jarecki and Keshishian, 1995). We live-imaged the formation and retraction of motoneuron filopodia during the innervation of muscles in intact embryos. Filopodia can newly

form, extend onto, and retract from off-target muscles during several hours of late embryogenesis, within the previously determined critical period. Live imaging of embryos revealed transient Ca^{2+} signals that became progressively regular and oscillatory at developing NMJs. In addition, the GCaMP signals were detected in filopodia that explored ectopic sites. Given previous evidence that episodic Ca^{2+} signaling at a specific low frequency is critical for the normal removal of ectopic contacts in a Sema2a-dependent fashion (Carrillo et al., 2010), we hypothesize that the regularly spaced, low-frequency Ca^{2+} transients observed in these ectopic contacts are a crucial part of a refinement mechanism.

There is good evidence that Ca^{2+} transients usually inhibit filopodial exploration. Increases in intracellular Ca^{2+} levels suppressed filopodial growth and elongation in cultured molluscan neurons (Cohan et al., 1987; Mattson and Kater, 1987). Also, in *Xenopus* neurons, *in vivo* imaging showed that high frequencies of Ca^{2+} transients in growth cones caused stalling and axon retraction (Gomez and Spitzer, 1999). One conclusion is that the rate of axon outgrowth is inversely related to the frequency of endogenous growth cone Ca^{2+} transients. Although reduced Ca^{2+} signaling could lead to neurite overgrowth and ectopic contacts, we observed no evidence of motoneuronal overgrowth in *cac*^{NT27} mutant embryos, where the number of synaptic boutons at native NMJs remained unaltered (Rieckhof et al., 2003). Therefore, we favor the hypothesis that the presence of ectopic contacts is due to alterations in the removal mechanism rather than to overgrowth.

Ca^{2+}-dependent regulation of chemorepulsion during refinement

Electrical activity plays a crucial role in the refinement of neural networks during development (Wiesel and Hubel, 1963). However, the mechanisms by which neural activity regulates the effects of guidance cues for proper neural circuit connectivity remain incompletely resolved. *In vitro* studies have shown that electrical activity modulates neural responses to chemotropic factors, such as netrin-1-induced attraction and myelin-associated glycoprotein-induced repulsion (Ming et al., 2001) in *Xenopus* neurons, as well as the repellent action of ephrin-A in mouse retinal ganglion cells (Nicol et al., 2007).

Our results indicate that ectopic contact removal depends on presynaptic Ca^{2+} influx through VGCCs. Consistent with this result, blockade of Ca^{2+} influx by Ca^{2+} channel blockers has been shown to suppress filopodial formation and growth cone elongation *in vitro* (Mattson and Kater, 1987). However, VGCCs are not the only source of the Ca^{2+} involved in growth cone behavior. In cultured *Xenopus* neurons, integrin-dependent, non–voltage-gated channels influence growth cone turning. Filopodial Ca^{2+} transients on one side of the growth cone promote turning from that side (Gomez et al., 2001). Similarly, the regulation of growth cone dynamics by axon guidance molecules, such as netrin-1, relies on other sources of Ca^{2+} signals. In cultured cortical neurons, netrin-1 promotes axon branching by localized Ca^{2+} transients (Tang and Kalil, 2005), in cultured *Xenopus* neurons netrin-1-induced turning responses depended on Ca^{2+} influx through plasma membrane Ca^{2+} channels, as well as Ca^{2+}-induced Ca^{2+} release from cytoplasmic stores (Hong et al., 2000). Although our results indicate a crucial role for VGCCs in ectopic contact removal, a role for Ca^{2+}-induced Ca^{2+} release in synaptic refinement in *Drosophila* remains untested.

An alternative hypothesis is that growth cone responses to attractive and repulsive signals are altered in *cac* and *Dmca1G*

mutants due to changes in the resting level of intracellular Ca^{2+}. Changes in growth cone Ca^{2+} concentrations are known to induce attraction as well as repulsion (Zheng, 2000; Wen et al., 2004), and a specific range of intracellular Ca^{2+} concentration regulates neurite outgrowth (Cohan et al., 1987; Mattson and Kater, 1987). Whereas a precise quantification of the Ca^{2+} concentrations in intact fly motoneuron growth cones remains to be determined, our results indicate that the frequency of Ca^{2+} events at the NMJ in late embryos is reduced in VGCC mutants.

A model for the mechanism underlying activity-dependent refinement

Calcium regulates various effectors (Clapham, 2007; Toth et al., 2016). Our results provide evidence for the role of the Ca^{2+}-dependent phosphatase CaN in refinement, a protein that is widely expressed in the nervous system (Klee et al., 1979, 1998). In flies, CaN regulates sleep (Nakai et al., 2011; Tomita et al., 2011), and CaN-LOF inhibits endocytosis of synaptic vesicles (Kuromi et al., 1997) and reduces bouton number (Wong et al., 2014). However, its role in activity-dependent synaptic refinement is not well established.

In vitro studies have also identified a role of CaN in the regulation of growth cone motility (Ferreira et al., 1993). Whereas blockade of CaN inhibits neurite outgrowth (Chang et al., 1995; Lautermilch and Spitzer, 2000; Graef et al., 2003), additional studies have shown that CaN promotes chemorepulsion in growth cones (Wen et al., 2004; Forbes et al., 2012). Our results are consistent with this idea, as CaN-LOF manipulations increased ectopic contact frequency whereas the CaN-GOF manipulations caused no connectivity defects.

In backgrounds with reduced Ca^{2+} levels, such as in cac^{NT27} mutants, we found that reducing CaN activity decreased ectopic frequency. One explanation involves the possibility that CaMKII activity is also reduced under low Ca^{2+} conditions. CaMKII function is required for proper refinement and may be inhibited by PP1 (Fig. 7E) (Shields et al., 1985). Because PP1 function is known to be promoted by CaN (Oliver and Shenolikar, 1998), reducing PP1 activation by decreasing CaN function (or by increasing PKA function; Fig. 6B,C) may increase CaMKII activity under low Ca^{2+} conditions, which would promote ectopic contact removal.

We propose a model where CaMKII is a key regulator for ectopic contact removal. CaMKII can act as a frequency decoder of Ca^{2+} transients (Deisseroth et al., 1995; Smedler and Uhlén, 2014). Furthermore, *in vitro* studies showed that CaMKII is required for neurite outgrowth (Goshima et al., 1993; Tang and Kalil, 2005) and suggest that CaMKII function promotes chemoattraction rather than chemorepulsion (Zheng et al., 1994; Wen et al., 2004; Forbes et al., 2012). However, our results show that CaMKII-LOF manipulations increase ectopic contact frequency. We hypothesize that CaMKII-dependent phosphorylation of molecules in the signaling pathway downstream of the Sema2a receptor, PlexinB, is required for ectopic contact removal. Furthermore, we observed that CaMKII function is required to be maintained within an optimal level for proper function, whereas CaMKII-LOF and -GOF manipulations both lead to miswiring. A similar optimal range has been previously described for intracellular cAMP levels, PKA, and PP1 (Vonhoff and Keshishian, 2017a). Here, we provide evidence for differential effects on refinement following CaMKII misregulation. Increased CaMKII function due to the expression of the constitutively active form T287D reduced the frequency of Ca^{2+} transients at the embryonic NMJ, likely by reducing membrane

excitability as observed in larval motoneurons (Park et al., 2002). By contrast, Ca^{2+} transient frequency was unaltered by the expression of the T287A construct, suggesting that decreased CaMKII function affects mechanisms other than excitability and Ca^{2+} influx, some of which may act downstream of PlexinB activation (Koropouli and Kolodkin, 2014). Consistently, introducing an additional source of Ca^{2+} influx rescued the T287A-dependent phenotype by a pattern adjusted to restore CaMKII activation at an optimal level. Because of the lack of autophosphorylation, CaMKII-T287A is predicted to be transiently activated every 30 s according to the native Ca^{2+} oscillation (Fig. 3). Our data suggest that adding a brief Ca^{2+} pulse every 5 min to the native pattern during the last hours of development might bring CaMKII-T287A activity levels to comparable ones of the WT-CaMKII. By contrast, no rescue of the phenotype was observed by introducing additional Ca^{2+} transients in animals with inhibited or constitutively active CaMKII.

We propose a model in which Ca^{2+} activates several effectors, such as the kinase CaMKII, the phosphatase CaN, and the adenylyl-cyclase Rutabaga, which elevates intracellular cAMP levels. Presynaptic cAMP is required to promote PKA function. In turn, PKA and CaN interact with PP1 to regulate CaMKII for proper refinement. These ideas are further explored in a review (Vonhoff and Keshishian, 2017b). These results provide a coherent picture of the links between neural activity, chemorepulsion, and the refinement of synaptic connectivity. A remaining task is to identify the manner in which these signals ultimately influence cytoskeletal dynamics and neurite retraction.

Notes

Supplemental material, time-lapse videos of embryonic growth cone behavior and Ca transients, can be viewed at the website link to the H.K. laboratory (http://mcdb.yale.edu/people/haig-keshishian). This material has not been peer reviewed.

References

Ackman JB, Burbridge TJ, Crair MC (2012) Retinal waves coordinate patterned activity throughout the developing visual system. Nature 490:219–225. CrossRef Medline

Ayoob JC, Yu HH, Terman JR, Kolodkin AL (2004) The *Drosophila* receptor guanylyl cyclase Gyc76C is required for semaphorin-1a-plexin A-mediated axonal repulsion. J Neurosci 24:6639–6649. CrossRef Medline

Ayoob JC, Terman JR, Kolodkin AL (2006) *Drosophila* Plexin B is a Sema-2a receptor required for axon guidance. Development 133:2125–2135. CrossRef Medline

Bennett D, Lyulcheva E, Alphey L, Hawcroft G (2006) Towards a comprehensive analysis of the protein phosphatase 1 interactome in *Drosophila*. J Mol Biol 364:196–212. CrossRef Medline

Berke B, Wittnam J, McNeill E, Van Vactor DL, Keshishian H (2013) Retrograde BMP signaling at the synapse: a permissive signal for synapse maturation and activity-dependent plasticity. J Neurosci 33:17937–17950. CrossRef Medline

Berridge MJ (2012) Calcium signalling remodelling and disease. Biochem Soc Trans 40:297–309. CrossRef Medline

Broadie KS, Bate M (1993) Development of the embryonic neuromuscular synapse of *Drosophila melanogaster*. J Neurosci 13:144–166. Medline

Campos-Ortega JA, Hartenstein V (1985) The embryonic development of *Drosophila melanogaster*. Berlin: Springer.

Carrillo RA, Olsen DP, Yoon KS, Keshishian H (2010) Presynaptic activity and CaMKII modulate retrograde semaphorin signaling and synaptic refinement. Neuron 68:32–44. CrossRef Medline

Catterall WA (2011) Voltage-gated calcium channels. Cold Spring Harb Perspect Biol 3:a003947. CrossRef Medline

Ceulemans H, Stalmans W, Bollen M (2002) Regulator-driven functional diversification of protein phosphatase-1 in eukaryotic evolution. Bioessays 24:371–381. CrossRef Medline

Chang HY, Takei K, Sydor AM, Born T, Rusnak F, Jay DG (1995) Asymmet-

ric retraction of growth cone filopodia following focal inactivation of calcineurin. Nature 376:686–690. CrossRef Medline

Chang TN, Keshishian H (1996) Laser Ablation of *Drosophila* embryonic motoneurons causes ectopic innervation of target muscle fibers. J Neurosci 16:5715–5726. Medline

Chiba A, Hing H, Cash S, Keshishian H (1993) Growth cone choices of *Drosophila* motoneurons in response to muscle fiber mismatch. J Neurosci 13:714–732. Medline

Clapham DE (2007) Calcium signaling. Cell 131:1047–1058. CrossRef Medline

Cohan CS, Connor JA, Kater SB (1987) Electrically and chemically mediated increases in intracellular calcium in neuronal growth cones. J Neurosci 7:3588–3599. Medline

Copf T (2014) Developmental shaping of dendritic arbors in *Drosophila* relies on tightly regulated intra-neuronal activity of protein kinase A (PKA). Dev Biol 393:282–297. CrossRef Medline

Crisp S, Evers JF, Fiala A, Bate M (2008) The development of motor coordination in *Drosophila* embryos. Development 135:3707–3717. CrossRef Medline

Deisseroth K, Bito H, Schulman H, Tsien RW (1995) Synaptic plasticity: a molecular mechanism for metaplasticity. Curr Biol 5:1334–1338. CrossRef Medline

Doll CA, Broadie K (2014) Impaired activity-dependent neural circuit assembly and refinement in autism spectrum disorder genetic models. Front Cell Neurosci 8:30. CrossRef Medline

Faul F, Erdfelder E, Lang AG, Buchner A (2007) G*Power 3: a flexible statistical power analysis program for the social, behavioral, and biomedical sciences. Behav Res Methods 39:175–191. CrossRef Medline

Ferreira A, Kincaid R, Kosik KS (1993) Calcineurin is associated with the cytoskeleton of cultured neurons and has a role in the acquisition of polarity. Mol Biol Cell 4:1225–1238. CrossRef Medline

Flavell SW, Greenberg ME (2008) Signaling mechanisms linking neuronal activity to gene expression and plasticity of the nervous system. Annu Rev Neurosci 31:563–590. CrossRef Medline

Forbes EM, Thompson AW, Yuan J, Goodhill GJ (2012) Calcium and cAMP levels interact to determine attraction versus repulsion in axon guidance. Neuron 74:490–503. CrossRef Medline

Gerber DJ, Hall D, Miyakawa T, Demars S, Gogos JA, Karayiorgou M, Tonegawa S (2003) Evidence for association of schizophrenia with genetic variation in the 8p21.3 gene, PPP3CC, encoding the calcineurin gamma subunit. Proc Natl Acad Sci U S A 100:8993–8998. CrossRef Medline

Gomez TM, Spitzer NC (1999) In vivo regulation of axon extension and pathfinding by growth cone calcium transients. Nature 397:350–355. CrossRef Medline

Gomez TM, Zheng JQ (2006) The molecular basis for calcium-dependent axon pathfinding. Nat Rev Neurosci 7:115–125. CrossRef Medline

Gomez TM, Robles E, Poo M, Spitzer NC (2001) Filopodial calcium transients promote substrate-dependent growth cone turning. Science 291:1983–1987. CrossRef Medline

Gorczyca MG, Phillis RW, Budnik V (1994) The role of tinman, a mesodermal cell fate gene, in axon pathfinding during the development of the transverse nerve in *Drosophila*. Development 120:2143–2152. Medline

Goshima Y, Ohsako S, Yamauchi T (1993) Overexpression of $Ca^{2+}/$calmodulin-dependent protein kinase II in Neuro2a and NG108-15 neuroblastoma cell lines promotes neurite outgrowth and growth cone motility. J Neurosci 13:559–567. Medline

Graef IA, Wang F, Charron F, Chen L, Neilson J, Tessier-Lavigne M, Crabtree GR (2003) Neurotrophins and netrins require calcineurin/NFAT signaling to stimulate outgrowth of embryonic axons. Cell 113:657–670. CrossRef Medline

Haghighi AP, McCabe BD, Fetter RD, Palmer JE, Hom S, Goodman CS (2003) Retrograde control of synaptic transmission by postsynaptic CaMKII at the *Drosophila* neuromuscular junction. Neuron 39:255–267. CrossRef Medline

Halpern ME, Chiba A, Johansen J, Keshishian H (1991) Growth cone behavior underlying the development of stereotypic synaptic connections in *Drosophila* embryos. J Neurosci 11:3227–3238. Medline

Hamada FN, Rosenzweig M, Kang K, Pulver SR, Ghezzi A, Jegla TJ, Garrity PA (2008) An internal thermal sensor controlling temperature preference in *Drosophila*. Nature 454:217–220. CrossRef Medline

Hanson MG, Landmesser LT (2004) Normal patterns of spontaneous activity are required for correct motor axon guidance and the expression of specific guidance molecules. Neuron 43:687–701. CrossRef Medline

Hanson MG, Milner LD, Landmesser LT (2008) Spontaneous rhythmic activity in early chick spinal cord influences distinct motor axon pathfinding decisions. Brain Res Rev 57:77–85. CrossRef Medline

Hong K, Nishiyama M, Henley J, Tessier-Lavigne M, Poo M (2000) Calcium signalling in the guidance of nerve growth by netrin-1. Nature 403:93–98. CrossRef Medline

Hu H, Marton TF, Goodman CS (2001) Plexin B mediates axon guidance in *Drosophila* by simultaneously inhibiting active Rac and enhancing RhoA signaling. Neuron 32:39–51. CrossRef Medline

Jarecki J, Keshishian H (1995) Role of neural activity during synaptogenesis in *Drosophila*. J Neurosci 15:8177–8190. Medline

Kanamori T, Kanai MI, Dairyo Y, Yasunaga K, Morikawa RK, Emoto K (2013) Compartmentalized calcium transients trigger dendrite pruning in *Drosophila* sensory neurons. Science 340:1475–1478. CrossRef Medline

Kater SB, Shibata A (1994) The unique and shared properties of neuronal growth cones that enable navigation and specific pathfinding. J Physiol Paris 88:155–163. CrossRef Medline

Katz LC, Shatz CJ (1996) Synaptic activity and the construction of cortical circuits. Science 274:1133–1138. CrossRef Medline

Klee CB, Crouch TH, Krinks MH (1979) Calcineurin: a calcium- and calmodulin-binding protein of the nervous system. Proc Natl Acad Sci U S A 76:6270–6273. CrossRef Medline

Klee CB, Ren H, Wang X (1998) Regulation of the calmodulin-stimulated protein phosphatase, calcineurin. J Biol Chem 273:13367–13370. CrossRef Medline

Kolodkin AL, Tessier-Lavigne M (2011) Mechanisms and molecules of neuronal wiring: a primer. Cold Spring Harb Perspect Biol 3:a001727. CrossRef Medline

Koropouli E, Kolodkin AL (2014) Semaphorins and the dynamic regulation of synapse assembly, refinement, and function. Curr Opin Neurobiol 27:1–7. CrossRef Medline

Kuromi H, Yoshihara M, Kidokoro Y (1997) An inhibitory role of calcineurin in endocytosis of synaptic vesicles at nerve terminals of *Drosophila* larvae. Neurosci Res 27:101–113. CrossRef Medline

Lautermilch NJ, Spitzer NC (2000) Regulation of calcineurin by growth cone calcium waves controls neurite extension. J Neurosci 20:315–325. Medline

Lee J, Wu CF (2010) Orchestration of stepwise synaptic growth by K^+ and Ca^{2+} channels in *Drosophila*. J Neurosci 30:15821–15833. CrossRef Medline

Liu YL, Fann CS, Liu CM, Chang CC, Yang WC, Hung SI, Yu SL, Hwang TJ, Hsieh MH, Liu CC, Tsuang MM, Wu JY, Jou YS, Faraone SV, Tsuang MT, Chen WJ, Hwu HG (2007) More evidence supports the association of PPP3CC with schizophrenia. Mol Psychiatry 12:966–974. CrossRef Medline

Matthes DJ, Sink H, Kolodkin AL, Goodman CS (1995) Semaphorin II can function as a selective inhibitor of specific synaptic arborizations. Cell 81:631–639. CrossRef Medline

Mattson MP, Kater SB (1987) Calcium regulation of neurite elongation and growth cone motility. J Neurosci 7:4034–4043. Medline

Meister M, Wong RO, Baylor DA, Shatz CJ (1991) Synchronous bursts of action potentials in ganglion cells of the developing mammalian retina. Science 252:939–943. CrossRef Medline

Menon KP, Carrillo RA, Zinn K (2013) Development and plasticity of the *Drosophila* larval neuromuscular junction. Wiley Interdiscip Rev Dev Biol 2:647–670. CrossRef Medline

Ming G, Henley J, Tessier-Lavigne M, Song H, Poo M (2001) Electrical activity modulates growth cone guidance by diffusible factors. Neuron 29:441–452. CrossRef Medline

Miyakawa T, Leiter LM, Gerber DJ, Gainetdinov RR, Sotnikova TD, Zeng H, Caron MG, Tonegawa S (2003) Conditional calcineurin knockout mice exhibit multiple abnormal behaviors related to schizophrenia. Proc Natl Acad Sci U S A 100:8987–8992. CrossRef Medline

Nakai Y, Horiuchi J, Tsuda M, Takeo S, Akahori S, Matsuo T, Kume K, Aigaki T (2011) Calcineurin and its regulator sra/DSCR1 are essential for sleep in *Drosophila*. J Neurosci 31:12759–12766. CrossRef Medline

Nicol X, Voyatzis S, Muzerelle A, Narboux-Nême N, Südhof TC, Miles R, Gaspar P (2007) cAMP oscillations and retinal activity are permissive for ephrin signaling during the establishment of the retinotopic map. Nat Neurosci 10:340–347. CrossRef Medline

Oliver CJ, Shenolikar S (1998) Physiologic importance of protein phosphatase inhibitors. Front Biosci 3:D961–D972. CrossRef Medline

Osterwalder T, Yoon KS, White BH, Keshishian H (2001) A conditional tissue-specific transgene expression system using inducible GAL4. Proc Natl Acad Sci U S A 98:12596–12601. CrossRef Medline

Park D, Coleman MJ, Hodge JJ, Budnik V, Griffith LC (2002) Regulation of neuronal excitability in Drosophila by constitutively active CaMKII. J Neurobiol 52:24–42. CrossRef Medline

Park SK, Sedore SA, Cronmiller C, Hirsh J (2000) Type II cAMP-dependent protein kinase-deficient Drosophila are viable but show developmental, circadian, and drug response phenotypes. J Biol Chem 275:20588–20596. CrossRef Medline

Penn AA, Riquelme PA, Feller MB, Shatz CJ (1998) Competition in retinogeniculate patterning driven by spontaneous activity. Science 279:2108–2112. CrossRef Medline

Pereanu W, Spindler S, Im E, Buu N, Hartenstein V (2007) The emergence of patterned movement during late embryogenesis of Drosophila. Dev Neurobiol 67:1669–1685. CrossRef Medline

Pulver SR, Pashkovski SL, Hornstein NJ, Garrity PA, Griffith LC (2009) Temporal dynamics of neuronal activation by Channelrhodopsin-2 and TRPA1 determine behavioral output in Drosophila larvae. J Neurophysiol 101:3075–3088. CrossRef Medline

Rieckhof GE, Yoshihara M, Guan Z, Littleton JT (2003) Presynaptic N-type calcium channels regulate synaptic growth. J Biol Chem 278:41099–41108. CrossRef Medline

Rosenberg SS, Spitzer NC (2011) Calcium signaling in neuronal development. Cold Spring Harb Perspect Biol 3:a004259. CrossRef Medline

Ruiz-Cañada C, Budnik V (2006) Introduction on the use of the Drosophila embryonic/larval neuromuscular junction as a model system to study synapse development and function, and a brief summary of pathfinding and target recognition. Int Rev Neurobiol 75:1–31. CrossRef Medline

Ryglewski S, Lance K, Levine RB, Duch C (2012) Ca(v)2 channels mediate low and high voltage-activated calcium currents in Drosophila motoneurons. J Physiol 590:809–825. CrossRef Medline

Schubert D, LaCorbiere M, Whitlock C, Stallcup W (1978) Alterations in the surface properties of cells responsive to nerve growth factor. Nature 273:718–723. CrossRef Medline

Sekar A, Bialas AR, de Rivera H, Davis A, Hammond TR, Kamitaki N, Tooley K, Presumey J, Baum M, Van Doren V, Genovese G, Rose SA, Handsaker RE, Daly MJ, Carroll MC, Stevens B, McCarroll SA (2016) Schizophrenia risk from complex variation of complement component 4. Nature 530:177–183. CrossRef Medline

Shields SM, Ingebritsen TS, Kelly PT (1985) Identification of protein phosphatase 1 in synaptic junctions: dephosphorylation of endogenous calmodulin-dependent kinase II and synapse-enriched phosphoproteins. J Neurosci 5:3414–3422. Medline

Sink H, Whitington PM (1991) Pathfinding in the central nervous system and periphery by identified embryonic Drosophila motor axons. Development 112:307–316. Medline

Smedler E, Uhlén P (2014) Frequency decoding of calcium oscillations. Biochim Biophys Acta 1840:964–969. CrossRef Medline

Sullivan KM, Rubin GM (2002) The Ca(2+)-calmodulin-activated protein phosphatase calcineurin negatively regulates EGF receptor signaling in Drosophila development. Genetics 161:183–193. Medline

Takeo S, Tsuda M, Akahori S, Matsuo T, Aigaki T (2006) The calcineurin regulator sra plays an essential role in female meiosis in Drosophila. Curr Biol 16:1435–1440. CrossRef Medline

Takeo S, Swanson SK, Nandanan K, Nakai Y, Aigaki T, Washburn MP, Florens L, Hawley RS (2012) Shaggy/glycogen synthase kinase 3beta and phosphorylation of Sarah/regulator of calcineurin are essential for completion of Drosophila female meiosis. Proc Natl Acad Sci U S A 109:6382–6389. CrossRef Medline

Tang F, Kalil K (2005) Netrin-1 induces axon branching in developing cortical neurons by frequency-dependent calcium signaling pathways. J Neurosci 25:6702–6715. CrossRef Medline

Tang G, Gudsnuk K, Kuo SH, Cotrina ML, Rosoklija G, Sosunov A, Sonders MS, Kanter E, Castagna C, Yamamoto A, Yue Z, Arancio O, Peterson BS, Champagne F, Dwork AJ, Goldman J, Sulzer D (2014) Loss of mTOR-dependent macroautophagy causes autistic-like synaptic pruning deficits. Neuron 83:1131–1143. CrossRef Medline

Tomita J, Mitsuyoshi M, Ueno T, Aso Y, Tanimoto H, Nakai Y, Aigaki T, Kume S, Kume K (2011) Pan-neuronal knockdown of calcineurin reduces sleep in the fruit fly, Drosophila melanogaster. J Neurosci 31:13137–13146. CrossRef Medline

Toth AB, Shum AK, Prakriya M (2016) Regulation of neurogenesis by calcium signaling. Cell Calcium 59:124–134. CrossRef Medline

Tully T, Quinn WG (1985) Classical conditioning and retention in normal and mutant Drosophila melanogaster. J Comp Physiol A 157:263–277. CrossRef Medline

Vonhoff F, Keshishian H (2017a) Cyclic nucleotide signaling is required during synaptic refinement at the Drosophila neuromuscular junction. Dev Neurobiol 77:39–60. CrossRef Medline

Vonhoff F, Keshishian H (2017b) Activity-dependent synaptic refinement: new insights from Drosophila. Front Syst Neurosci 11:23. CrossRef

Wen Z, Guirland C, Ming GL, Zheng JQ (2004) A CaMKII/calcineurin switch controls the direction of Ca(2+)-dependent growth cone guidance. Neuron 43:835–846. CrossRef Medline

White BH, Osterwalder TP, Yoon KS, Joiner WJ, Whim MD, Kaczmarek LK, Keshishian H (2001) Targeted attenuation of electrical activity in Drosophila using a genetically modified K+ channel. Neuron 31:699–711. CrossRef Medline

Wiesel TN, Hubel DH (1963) Effects of visual deprivation on morphology and physiology of cells in the cats lateral geniculate body. J Neurophysiol 26:978–993. Medline

Winberg ML, Mitchell KJ, Goodman CS (1998) Genetic analysis of the mechanisms controlling target selection: complementary and combinatorial functions of netrins, semaphorins, and IgCAMs. Cell 93:581–591. CrossRef Medline

Wong CO, Chen K, Lin YQ, Chao Y, Duraine L, Lu Z, Yoon WH, Sullivan JM, Broadhead GT, Sumner CJ, Lloyd TE, Macleod GT, Bellen HJ, Venkatachalam K (2014) A TRPV channel in Drosophila motor neurons regulates presynaptic resting Ca2+ levels, synapse growth, and synaptic transmission. Neuron 84:764–777. CrossRef Medline

Worrell JW, Levine RB (2008) Characterization of voltage-dependent Ca2+ currents in identified Drosophila motoneurons in situ. J Neurophysiol 100:868–878. CrossRef Medline

Wu Z, Sweeney LB, Ayoob JC, Chak K, Andreone BJ, Ohyama T, Kerr R, Luo L, Zlatic M, Kolodkin AL (2011) A combinatorial semaphorin code instructs the initial steps of sensory circuit assembly in the Drosophila CNS. Neuron 70:281–298. CrossRef Medline

Zheng JQ (2000) Turning of nerve growth cones induced by localized increases in intracellular calcium ions. Nature 403:89–93. CrossRef Medline

Zheng JQ, Poo MM (2007) Calcium signaling in neuronal motility. Annu Rev Cell Dev Biol 23:375–404. CrossRef Medline

Zheng JQ, Felder M, Connor JA, Poo MM (1994) Turning of nerve growth cones induced by neurotransmitters. Nature 368:140–144. CrossRef Medline

Zito K, Parnas D, Fetter RD, Isacoff EY, Goodman CS (1999) Watching a synapse grow: noninvasive confocal imaging of synaptic growth in Drosophila. Neuron 22:719–729. CrossRef Medline